



## GATA1-Deficient Dendritic Cells Display Impaired CCL21-Dependent Migration toward Lymph Nodes Due to Reduced Levels of Polysialic Acid

This information is current as of February 26, 2022.

Maaïke R. Scheenstra, Iris M. De Cuyper, Filipe Branco-Madeira, Pieter de Bleser, Mirjam Kool, Marjolein Meinders, Mark Hoogenboezem, Erik Mul, Monika C. Wolkers, Fiamma Salerno, Benjamin Nota, Yvan Saeys, Sjoerd Klarenbeek, Wilfred F. J. van IJcken, Hamida Hammad, Sjaak Philipsen, Timo K. van den Berg, Taco W. Kuijpers, Bart N. Lambrecht and Laura Gutiérrez

*J Immunol* 2016; 197:4312-4324; Prepublished online 4 November 2016;  
doi: 10.4049/jimmunol.1600103  
<http://www.jimmunol.org/content/197/11/4312>

**Supplementary Material** <http://www.jimmunol.org/content/suppl/2016/11/04/jimmunol.1600103.DCSupplemental>

**References** This article **cites 80 articles**, 30 of which you can access for free at:  
<http://www.jimmunol.org/content/197/11/4312.full#ref-list-1>

**Why *The JI*? Submit online.**

- **Rapid Reviews! 30 days\*** from submission to initial decision
- **No Triage!** Every submission reviewed by practicing scientists
- **Fast Publication!** 4 weeks from acceptance to publication

*\*average*

**Subscription** Information about subscribing to *The Journal of Immunology* is online at:  
<http://jimmunol.org/subscription>

**Permissions** Submit copyright permission requests at:  
<http://www.aai.org/About/Publications/JI/copyright.html>

**Email Alerts** Receive free email-alerts when new articles cite this article. Sign up at:  
<http://jimmunol.org/alerts>



# GATA1-Deficient Dendritic Cells Display Impaired CCL21-Dependent Migration toward Lymph Nodes Due to Reduced Levels of Polysialic Acid

Maaïke R. Scheenstra,\* Iris M. De Cuyper,\* Filipe Branco-Madeira,<sup>†,‡</sup> Pieter de Bleser,<sup>§</sup> Mirjam Kool,<sup>†</sup> Marjolein Meinders,\* Mark Hoogenboezem,<sup>¶</sup> Erik Mul,<sup>¶</sup> Monika C. Wolkers,<sup>||</sup> Fiamma Salerno,<sup>||</sup> Benjamin Nota,\* Yvan Saeys,<sup>§</sup> Sjoerd Klarenbeek,<sup>#</sup> Wilfred F. J. van IJcken,\*\* Hamida Hammad,<sup>†,‡</sup> Sjaak Philipsen,<sup>††</sup> Timo K. van den Berg,\* Taco W. Kuijpers,\*<sup>‡,‡</sup> Bart N. Lambrecht,<sup>†,‡,§§</sup> and Laura Gutiérrez\*,<sup>¶¶</sup>

Dendritic cells (DCs) play a pivotal role in the regulation of the immune response. DC development and activation is finely orchestrated through transcriptional programs. GATA1 transcription factor is required for murine DC development, and data suggest that it might be involved in the fine-tuning of the life span and function of activated DCs. We generated DC-specific *Gata1* knockout mice (*Gata1*-KO<sup>DC</sup>), which presented a 20% reduction of splenic DCs, partially explained by enhanced apoptosis. RNA sequencing analysis revealed a number of deregulated genes involved in cell survival, migration, and function. DC migration toward peripheral lymph nodes was impaired in *Gata1*-KO<sup>DC</sup> mice. Migration assays performed in vitro showed that this defect was selective for CCL21, but not CCL19. Interestingly, we show that *Gata1*-KO<sup>DC</sup> DCs have reduced polysialic acid levels on their surface, which is a known determinant for the proper migration of DCs toward CCL21. *The Journal of Immunology*, 2016, 197: 4312–4324.

Dendritic cells (DCs) are key initiators and regulators of the immune response (1). Two major types of DCs have been defined in mouse and human in the steady-state, that is, conventional DC (cDCs) and plasmacytoid DCs. Under inflammatory conditions, yet another type of DC, so-called inflammatory DC, derives from circulating monocytes (2). In mice, cDCs can be further subdivided into CD8a<sup>+</sup>CD24<sup>+</sup>Xcr1<sup>+</sup> cDCs (also called cDC1) and CD11b<sup>+</sup>Sirp-α<sup>+</sup> cDCs (also called cDC2) (3–8). Immature DCs express several receptors for pathogen-associated molec-

ular patterns, such as TLRs, which can induce the activation of DCs when recognizing their ligand. Activated DCs migrate to the lymph nodes to activate T and B cells by Ag presentation on MHC class I (MHC-I) or MHC-II (9). Migratory DCs in the lymph nodes can be distinguished from resident cDCs by their higher MHC-II expression (2, 5, 9). Both cDC subtypes can activate CD4<sup>+</sup> T cells through MHC-II in the lymphoid organs. In addition, CD8a<sup>+</sup> cDCs are specialized to cross-present Ag on the MHC-I molecule, and thereby are capable of priming CD8<sup>+</sup> cytotoxic T cells (3, 5, 9–11).

\*Department of Blood Cell Research, Sanquin Research and Landsteiner Laboratory, Academic Medical Center, University of Amsterdam, Amsterdam 1066CX, the Netherlands; <sup>†</sup>Laboratory of Immunoregulation, VIB, Ghent 9052, Belgium; <sup>‡</sup>Department of Internal Medicine, Ghent University, Ghent 9000, Belgium; <sup>§</sup>Data Mining and Modeling for Biomedicine, Department of Biomedical Molecular Biology, VIB Inflammation Research Center, Ghent University, Ghent 9052, Belgium; <sup>¶</sup>Department of Molecular Cell Biology, Sanquin Research and Landsteiner Laboratory, Academic Medical Center, University of Amsterdam, Amsterdam 1066CX, the Netherlands; <sup>||</sup>Department of Hematopoiesis, Sanquin Research and Landsteiner Laboratory, Academic Medical Center, University of Amsterdam, Amsterdam 1066CX, the Netherlands; <sup>#</sup>Experimental Animal Pathology, The Netherlands Cancer Institute, Amsterdam 1066CX, the Netherlands; \*\*Center for Biomics, Erasmus MC, Rotterdam 3015 CN, the Netherlands; <sup>††</sup>Department of Cell Biology, Erasmus MC, Rotterdam 3015 CN, the Netherlands; <sup>‡‡</sup>Department of Pediatric Hematology, Immunology and Infectious Disease, Emma Children's Hospital, Academic Medical Center, University of Amsterdam, Amsterdam 1105AZ, the Netherlands; <sup>§§</sup>Department of Pulmonary Medicine, Erasmus MC, Rotterdam 3015 CN, the Netherlands; and <sup>¶¶</sup>Departamento de Hematología, Hospital Clínico San Carlos, Instituto de Investigación Sanitaria San Carlos, Madrid 28040, Spain

ORCID: 0000-0001-8862-8000 (I.M.D.C.); 0000-0001-5245-9735 (F.B.-M.); 0000-0003-4762-8770 (P.d.B.); 0000-0003-1436-3876 (M.K.); 0000-0002-7124-0832 (M.M.); 0000-0002-8234-9972 (E.M.); 0000-0003-3242-1363 (M.C.W.); 0000-0003-1634-947X (F.S.); 0000-0001-7500-5760 (B.N.); 0000-0002-0415-1506 (Y.S.); 0000-0002-1891-1940 (S.K.); 0000-0002-0421-8301 (W.F.J.v.I.); 0000-0002-3690-1201 (S.P.); 0000-0001-8443-900X (L.G.).

Received for publication January 21, 2016. Accepted for publication September 29, 2016.

This work was supported by a VENI grant from the Netherlands Scientific Organization (Grant VENI 863.09.012 to L.G.), an Ramón y Cajal fellowship from the Spanish Ministerio de Economía y Competitividad (Grant RYC-2013-12587 to L.G.), Landsteiner Foundation for Blood Transfusion Research Grant LSBR 1040

(to S.P.), Netherlands Scientific Organization Grant ZonMW TOP 40-00812-98-12128 (to S.P.), and Seventh Framework Programme, European Union research and development funding program EU fp7 THALAMOSS 306201 (to S.P.).

M.R.S. and L.G. designed and performed experiments, analyzed data, and wrote the manuscript; I.M.D.C. performed experiments, analyzed data, and revised the manuscript; F.B.-M. performed experiments and revised the manuscript; W.F.J.v.I. performed RNA sequencing (RNA-Seq); B.N. performed RNA-Seq analysis; P.d.B. and Y.S. performed RNA-Seq and principal component analysis; M.K., M.M., M.H., E.M., F.S., and S.K. performed experiments; M.C.W. and H.H. designed experiments and revised the manuscript; S.P., T.K.v.d.B., T.W.K., and B.N.L. participated in discussions, designed experiments, and revised the manuscript.

The data presented in this article have been submitted to the Gene Expression Omnibus under accession number GSE69969.

Address correspondence and reprint requests to Dr. Laura Gutiérrez, Department of Hematology, Hospital Clínico San Carlos, Instituto de Investigación Sanitaria San Carlos, Profesor Martín Lagos s/n, Room 1578, First Floor, Madrid 28040, Spain. E-mail address: lgutierrezg@salud.madrid.org

The online version of this article contains supplemental material.

Abbreviations used in this article: BAC, bacterial artificial chromosome; BM-DC, bone marrow-derived DC; cDC, conventional DC; Ct, cycle threshold; DC, dendritic cell; *Gata1*-KO<sup>DC</sup>, DC-specific *Gata1* knockout mice; GO, Gene Ontology; IPA, Ingenuity Pathway Analysis; KO, knockout; MHC-I, MHC class I; PCA, principal component analysis; PIpropidium iodide, peripheral lymph node; PLN, peripheral lymph node; PSA, polysialic acid; RNA-Seq, RNA sequencing; WT, wild type; WT<sup>lox</sup>, *Gata1*-lox male littermate; WT<sup>Cre</sup>, CD11cCre male not bearing *Gata1*-lox allele.

Copyright © 2016 by The American Association of Immunologists, Inc. 0022-1767/16/\$30.00

The development of DCs from hematopoietic progenitors is tightly regulated by transcriptional programs (12, 13). The role of several transcription factors in DC development has been studied using genetically modified mice and by reconstitution assays (14). Several transcription factors have been found to regulate DC subset differentiation. Mice deficient for IRF2, IRF4, KLF4, or RelB have a strong reduction in the CD11b<sup>+</sup> cDC subset (15–18), whereas IRF8 and Batf3 deficiency results in a strong reduction in the CD8a<sup>+</sup> cDC subset (19, 20). IRF4 and IRF8 are important for the *in vitro* generation of bone marrow (BM)-derived DCs (BM-DCs), either in the presence of GM-CSF or Flt3L (20). Other transcription factors, such as SPI1 (also known as PU.1), are involved in the development and differentiation of both cDC subsets. PU.1 regulates *Flt3* expression, which is essential for DC development (21). Loss of PU.1 in the DC lineage results in a general cDC defect, with the CD8<sup>+</sup> cDC subtype being more severely affected than the CD11b<sup>+</sup> cDC subtype (14, 21, 22). GATA1 transcription factor, which exerts functions antagonistic to PU.1, is expressed in both cDCs and plasmacytoid DCs (23) and is required for proper differentiation (24). GATA1 belongs to the GATA family of transcription factors, characterized by two zinc finger domains for DNA binding to the GATA consensus sequence (WGATAR), as well as motifs for protein–protein interactions (25). GATA1 is essential for differentiation of erythrocytes and megakaryocytes (25–27). In these lineages, GATA1 regulates the transcription of cell-specific and antiapoptotic genes (26, 28–31).

Not much is known yet about the role of GATA1 in DCs. GATA1 was found to be important for the lineage separation between DCs and macrophages, being indispensable for DC commitment and differentiation from progenitors (24). It was also observed that GATA1 is required for DC survival and function, in particular upon LPS stimulation of GM-CSF-cultured BM-DCs. In humans, DC differentiation from blood monocytes was reported to coincide with the upregulation of GATA1 expression as a crucial cell fate factor for the dichotomy between Langerhans cells and DC lineage development (26). The closely related GATA2 transcription factor has been recently linked to DC differentiation. Patients carrying mutations in the *GATA2* gene present with MonoMac disease (an autosomal dominant immunodeficiency caused by the lack of monocytes, DCs, B cells, and NK cells) and are prone to development of myelodysplasia and/or leukemia (32). In addition, conditional *GATA2* loss in mice results in severely reduced DC numbers (33).

In this study, we dissect the role of GATA1 in DCs using a DC-specific *Gata1* knockout (KO) mouse (*Gata1*-KO<sup>DC</sup>) model. We found that *Gata1*-KO<sup>DC</sup> mice display a decrease in the splenic DC compartment. RNA sequencing (RNA-Seq) revealed a number of deregulated genes involved in cell survival, migration, and function in *Gata1*-KO<sup>DC</sup> DCs. Interestingly, we observed impaired DC migration toward the lymph nodes in *Gata1*-KO<sup>DC</sup> mice upon LPS treatment and in aging mice. The migration defect was CCL21 dependent. This phenomenon could be explained by reduced polysialic acid (PSA) surface expression levels in LPS-stimulated *Gata1*-KO<sup>DC</sup> DCs.

## Materials and Methods

### Mice

Mice bearing a modified *Gata1* allele flanked with loxP sites (34) were crossed with mice expressing a constitutively active Cre recombinase under the *CD11c* promoter (*CD11c*Cre [bacterial artificial chromosome (BAC)] from the Jackson Laboratory [B6.Cg-Tg(*Itgax*-cre)]1-1Reiz/J, strain 008068] (35). Because the *Gata1* gene is X-linked, only *Gata1*-lox/*CD11c*Cre (BAC) males were used to obtain DC-specific pancellular *Gata1* recombination, and we named them *Gata1*-KO<sup>DC</sup>. *Gata1*-lox male littermates (WT<sup>lox</sup>) were used as controls. In addition, and to be able to sort an enriched population of recombined DCs for RNA-Seq, we used the R26R-RG reporter strain (provided by S. Aizawa). These mice bear a conditional

reporter transgene at the *Rosa26* locus, and upon Cre recombination they express nuclear-mCherry and surface-EGFP (36). We crossed R26R-RG mice with *Gata1*-lox/*CD11c*Cre (BAC) mice, and used R26R-RG/*Gata1*-lox/*CD11c*Cre (R26R-RG/*Gata1*-KO<sup>DC</sup>) and R26R-RG/*CD11c*Cre (R26R-RG/*CD11c*Cre males not bearing *Gata1*-lox allele [WT<sup>Cre</sup>]) mice for the generation of DCs in culture as specified later.

Mice were used between 8 and 16 wk of age, unless stated otherwise. When indicated, LPS (Sigma) was administered (5 µg/mouse) via i.v. injection, and mice were sacrificed after 24 h for further analysis.

Mice were kept specified pathogen-free with free access to food and water at all times, under the guidelines for animal experimentation approved by the animal ethical comity of the Netherlands Cancer Institute (NKI, Amsterdam, the Netherlands), Erasmus MC, and VIB.

### Mouse BM-DC culture

BM was obtained by crushing the femur and tibia of both legs, after which the cells were filtered through a 40-µm filter (BD Biosciences) to obtain a single-cell suspension. Cells were cultured at a density of  $0.5 \times 10^6$ /ml in RPMI 1640 (Life Technologies) supplemented with 5% heat-inactivated FCS, 1% penicillin/streptomycin, 5 µM 2-ME, and 20 ng/ml GM-CSF (Peprotech). A total of 0.5 µg/ml LPS (Santa Cruz Biotechnology) was added to the cells at day 7, and the cells were harvested for further analysis at days 8 and 10.

### Cell purification and flow cytometry

Blood was drawn by heart puncture and collected in heparin-coated vials (Sarstedt, Nümbrecht, Germany). The scil Vet abc Plus+ automated hemocytometer was used to determine standard blood parameters. Spleen and lymph nodes were taken from the mice and digested in RPMI 1640 (Life Technologies), supplemented with 1.5 Wünsch activity units/ml Liberase TL grade (Roche, U.K.), 0.5 µg/ml Aggrastat (MSD), and 2 Kunitz units/ml DNase (Sigma) for 30 min at 37°C. Single-cell suspensions were made using a 40-µm filter (BD Biosciences), and the cells were washed with PBS/0.5 mM of EDTA. Blood and spleen samples were treated with an isotonic ammonium chloride buffer for 5 min at 4°C to lyse the erythrocytes, after which lysis buffer was washed away with PBS.

Cells (from organs and cultured BM-DCs) were stained for different markers (for Abs used, see Table I). In addition, cells were incubated in a HEPES buffer containing 2.5 mM of CaCl<sub>2</sub> for Annexin V and propidium iodide (PI) staining. Samples were measured on a BD FACSCanto II or BD FACSFortessa flow cytometer (BD Biosciences) and analyzed with FlowJo software.

### RNA extraction

For RNA-Seq analysis, BM-derived GM-CSF DCs from R26R-RG/*Gata1*-KO<sup>DC</sup> and R26R-RG/WT<sup>Cre</sup> mice were used nonstimulated and stimulated with LPS at day 7 as described earlier. At day 10, steady-state DCs and LPS-stimulated DCs were harvested and sorted for GFP<sup>+</sup>/mCherry<sup>+</sup> cells. This strategy allowed enriching for DCs that had undergone Cre-mediated recombination for both the WT<sup>Cre</sup> and the R26R-RG/*Gata1*-KO<sup>DC</sup> cultures. Total RNA was extracted from the sorted DCs using the RNeasy-plus mini kit (Qiagen).

### RNA-Seq

RNA-Seq was performed according to manufacturer's instructions (Illumina) using the TruSeq RNA sample prep kit v2. In brief, polyA-containing mRNA molecules were purified using oligo-dT attached to magnetic beads. After purification, the mRNA was fragmented into ~200-bp fragments using divalent cations under elevated temperature. The cleaved RNA fragments were copied into first-strand cDNA using reverse transcriptase and random primers. This was followed by second-strand synthesis using DNA polymerase I and RNase H treatment. These cDNA fragments were end repaired, a single A base was added, and Illumina adaptors were ligated. The products were purified and size selected on gel and enriched by PCR. The PCR products were purified by QIAquick PCR purification and used for cluster generation according to the Illumina cluster generation protocols. The samples ( $n = 2$  for every condition) were sequenced for 36 bp on a HiSeq2000 and demultiplexed using Narwhal (37). The reads were aligned using TopHat version 2.0.8 (38) against the University of California, Santa Cruz Genome Browser mm10 reference genome, using Ensemblgenes.gtf version 73 (39). For RNA of R26R-RG/*Gata1*-KO<sup>DC</sup> DCs, we obtained an average of 17.1 million reads for steady-state condition and 13.1 million reads for LPS-stimulated condition, of which 93.7 and 91.3% aligned back, respectively, to the reference genome. For WT<sup>Cre</sup> DC samples, we obtained an average of 17.3 million reads for steady-state condition and 18.9 million reads for LPS-stimulated condition, with 93.2 and 93.3% alignment, respectively (Supplemental Fig. 2B). The data were submitted to GEO (accession number GSE69969).



### RNA-Seq data analysis

For all 23,420 University of California, Santa Cruz Genome Browser mm10 annotated genes, the reads were counted that aligned to the exonic regions using “feature Counts” from Subread (version 1.4.3) (40). Differential gene expression assessment was done in the R environment (version 3.1.1) with edgeR (version 3.6.8) (41), as earlier described (42). The following group comparisons were made: R26R-RG|Gata1-KO<sup>DC</sup> versus WT<sup>Cre</sup> under steady-state condition, and R26R-RG|Gata1-KO<sup>DC</sup> versus WT<sup>Cre</sup> under LPS condition. The *p* values were adjusted for multiple testing using FDR control (43), and adjusted *p* < 0.05 was considered significant. Two-dimensional hierarchical clustering was done with significant genes using only default settings of the “heatmap.2” function from the gplots (version 2.16) R package, using log2-transformed reads per kilobase per million data. The normalized gene expression data were scaled by row (Z-score). Gene Ontology (GO) gene set enrichment analyses were carried out with the Goseq R package (version 1.16.2) (44). Enrichment of GO terms was assessed in each list of differentially expressed genes per contrast separately, taking length bias into account. The derived *p* values were adjusted for multiple testing using Bonferroni correction, and adjusted *p* < 0.05 was considered significant.

HOMER software suite was used, with default settings, to identify enrichment of known motifs in promoters of differentially regulated genes (45).

Principal component analysis (PCA) was performed using Fastq files that were equally processed with fastqc version 0.11.2 (46) and trimmomatic v0.33 (47). Mapping to the reference genome was done using TopHat2 v2.0.10 (38), and filtering was done with samtools v0.1.19 (48). Counting reads in features was done with htseq-count (49). PCA analysis was performed in R. ComBat was used to correct for batch effects (50). Data sets used are publicly available: cultured BM-derived M-CSF macrophages (GSM1520422 and GSM1520423) and cultured BM-derived GM-CSF DCs, treated or not with LPS (GSM1620172, GSM624287, and GSM722533).

### Quantitative RT-PCR

Total RNA was extracted from cultured WT<sup>lox</sup> and KO<sup>DC</sup> cultured DCs with the RNeasy-plus mini kit (Qiagen) used according to the manufacturer's instructions. cDNA was synthesized with Superscript III RT (Invitrogen). Custom-made primers were used to amplify desired transcripts with SYBR green as a detection method with the StepOnePlus real-time PCR system (Applied Biosystems): *Gata1*, fw 5'-CAGTCCTTCTTCTCTCCAC-3' and rev 5'-GCTCCACAGTTTCACACACT-3'. Input was normalized using housekeeping genes (*Hprt*: fw 5'-AGCCTAAGATGAGCGCAAGT-3' and rev 5'-ATGGCGACAGGACTAGAACA-3'; *Ubc*: fw 5'-AGGTCAAACAGGAAGACAGACGTA-3' and rev 5'-TCACACCCAAGAA-CAAGACA-3'; and *Gapdh*: fw 5'-CCTGCCAAGTATGATGACAT-3' and rev 5'-GTCCTCAGTGTAGCCCAAG-3'), and relative expression was calculated using the cycle threshold (Ct) value method ( $\Delta\Delta C_t$ ); that is, relative expression =  $2^{-\Delta C_t}$ , where  $\Delta C_t = C_{t, \text{target gene}} - \text{average } C_{t, \text{housekeeping genes}}$  (51).

### Protein extraction and Western blotting

Naive (CD44<sup>low</sup>) CD4<sup>+</sup> and CD8<sup>+</sup> T cells were sorted from wild type (WT) mouse spleens, and  $5 \times 10^6$  cells were lysed in 100  $\mu$ l of sample lysis buffer. BM-DCs from WT<sup>lox</sup> and KO<sup>DC</sup> mice were lysed with radioimmunoprecipitation assay buffer (10 mM of Tris-HCL [pH 8], 1 mM of EDTA, 0.5 mM of EGTA, 140 mM of NaCl, 1% Triton X-100, 0.1% NaDOC, 0.1% SDS) containing protease inhibitors. As control for GATA1 expression, we used I/11 mouse erythroid cell line; for protein extraction,  $1 \times 10^6$  cells were lysed in 100  $\mu$ l of sample lysis buffer. Protein concentrations were measured with BCA Protein Assay Reagent (Thermo Scientific, Rockford, IL). Protein samples were separated using a 10% SDS-polyacrylamide gel, after which they were transferred to a polyvinylidene difluoride membrane (Millipore, Billerica, MA). Membranes were labeled with GATA1 (M20 or N6) Abs and thereafter with anti-goat or anti-rat IgG-HRP. Pierce ECL Western blotting substrate was used to visualize HRP. Super RX films were developed in the medical film processor SRX-101A (Konic Minolta, Tokyo, Japan). As loading control, GAPDH (Merck Millipore, Darmstadt, Germany) was used, followed by anti-mouse-IgG-IRDye 800CW-conjugated Ab (LI-COR, Lincoln, NE) and visualized using LI-COR Odyssey Western blot detection system (Westburg, Leusden, the Netherlands). Protein levels were quantified using ImageJ.

### Transwell migration

A total of  $2 \times 10^6$  cultured WT<sup>lox</sup> or KO<sup>DC</sup> DCs was labeled with calcein-AM (Invitrogen) for 30 min at 37°C in HEPES-buffered saline solution (134 mM of NaCl, 0.34 mM of Na<sub>2</sub>HPO<sub>4</sub>, 2.9 mM of KCl, 12 mM of NaHCO<sub>3</sub>, 20 mM of HEPES, 5 mM of glucose, 1 mM of MgCl<sub>2</sub> [pH 7.3]). A total of  $4 \times 10^5$  cells was added in the upper well of Transwell on a

FluoroBlock filter (8.0- $\mu$ m pores; Corning). The filters were placed in a 24-well plate, which contained 200 ng/ml CCL19 or CCL21 (BioLegend). The plates were placed in the F200-pro plate reader (Tecan, Männedorf, Switzerland), which was set to 37°C. Fluorescence was measured every 10 min for 3 h with an excitation wavelength of 485 nm and an emission wavelength of 535 nm.

### CCL21 binding assay

A total of  $1 \times 10^5$  cultured WT<sup>lox</sup> or KO<sup>DC</sup> BM-DCs was resuspended in HEPES buffer saline solution, as described earlier, and placed in a 96-well plate. Cells were incubated for 30 min with 20 ng/ml CCL21 on ice, after which the cells were fixed and permeabilized, using the fix/perm kit from BD Biosciences. Cells were incubated with CCL21 Ab (R&D Systems) for 30 min on ice in perm/wash buffer, after which cells were incubated with a FITC-labeled anti-goat Ab (Life Technologies). Samples were measured on a BD FACSCanto II and analyzed with FlowJo software.

### Statistical analysis

Results are presented as the mean  $\pm$  SEM. Statistical significance was assessed with two-sided Student *t* tests, as calculated with GraphPad Prism software, version 6.02.

## Results

### GATA1 loss in DCs results in a reduction of the splenic DC compartment

*Gata1*-lox mice (34) were crossed with CD11c-Cre mice (35) to generate DC-specific *Gata1* KO mice (*Gata1*-KO<sup>DC</sup>). CD11c-Cre mice have been previously characterized by Caton et al. (35), and from this study it was reported that the recombination efficiency in DCs is 96% using a R26-EYFP reporter mouse. In addition, “leaky” recombination in other lineages was also reported, for example, 0.3% in granulocytes, 6% in T cells, 5% in B cells, and 12% in NK cells. Of these, GATA1 is expressed only in a subset of granulocytes, that is, in eosinophils, whereas it is undetectable in lymphocytes (24).

We measured the complete blood counts of *Gata1*-KO<sup>DC</sup> mice and WT littermates (WT<sup>lox</sup>) on a Scil Vet abc Plus+ Hematology analyzer. RBC and platelet counts, lineages that require *Gata1* expression (25), were in the normal range in both WT<sup>lox</sup> and *Gata1*-KO<sup>DC</sup> mice (Fig. 1A), indicating no recombination leakage in the megakaryocyte/erythroid lineages.

*Gata1*-KO<sup>DC</sup> mice presented with a mild reduction in WBC counts, which was caused by a reduction in lymphocytes, because there were no differences in granulocyte numbers and only a mild significant increase in monocytes in *Gata1*-KO<sup>DC</sup> mice (Fig. 1A). By flow cytometry, we dissected the lymphocyte populations in the blood and identified a reduction in T cells, which was specifically due to a decrease in CD4<sup>+</sup> T cells and not CD8<sup>+</sup> T cells (Fig. 1B) (see Table I for a list of Abs used). The T cell lineage in other organs was not affected, nor was the B cell lineage (data not shown). Because the majority of blood lymphocytes are B cells, we sorted splenic CD4<sup>+</sup> and CD8<sup>+</sup> T cells from WT animals to analyze GATA1 expression (Supplemental Fig. 1A). We were unable to detect full-length GATA1, and observed very low levels of the short GATA1 isoform in both T cell subsets. All together, these results suggest that the specific reduction of CD4<sup>+</sup> T cells in the blood is probably not due to leaky recombination in the T cell lineage.

We next analyzed the cDC subtypes in different lymphoid organs. First, we selected non-B cells after which DCs were gated based on CD11c and MHC-II expression (Fig. 1C). We found a significant reduction of cDCs in the spleen of *Gata1*-KO<sup>DC</sup> mice, whereas no differences were found in the blood and the lymph nodes (Fig. 1D). The splenic cDCs were further subdivided into CD11b<sup>+</sup> and CD8<sup>+</sup> subsets (Fig. 1C), and we found that the reduction of cDCs in the spleen was due to a decrease of both subsets in *Gata1*-KO<sup>DC</sup> mice, although CD11b<sup>+</sup> DCs were more strongly reduced (Fig. 1D).

Table I. List of Abs

Ag	Label	Clone	Supplier
Annexin V	FITC		BD Pharmingen
CCL21	—		R&D Systems
CCR7	PE	4B12	eBioscience
CD3e	eFluor780	17A2	eBioscience
CD4	Allophycocyanin	RM4-5	BD Pharmingen
CD4	PE	GK1.5	eBioscience
CD8a	PE-Cy7/PerCP-Cy5.5	53-6.7	BD Pharmingen
CD11b	Allophycocyanin-Cy7	M1/70	BD Pharmingen
CD11c	PE	HL3	BD Pharmingen
CD19	PE-Cy7	eBio1D3	eBioscience
CD24	Pacific blue	M1/69	eBioscience
CD40	FITC	3/23	BD Pharmingen
CD44	PerCP-Cy5.5/eV450-Pacific blue	IM7	eBioscience
CD86	PerCP	GL-1	BioLegend
GATA1	—	M-20	Santa Cruz
GATA1	—	N6	Santa Cruz
GAPDH	—	6C5	Merck Millipore
MHC-II	FITC	M5/114.15.2	eBioscience
PI	—		BD Pharmingen
PSA-NCAM <sup>a</sup>	PE	2-2B	Miltenyi Biotec
Anti-goat IgG	AF488		Life Technologies
Anti-goat IgG	HRP		Thermo Fisher
Anti-mouse IgG	IRDye 800CW		Li-Cor
Anti-rat IgG	HRP		Dako

<sup>a</sup>From supplier datasheet (<http://www.miltenyibiotec.com/>; order no. 130-093-274; date last accessed: October 2016): “The Anti-PSA-NCAM antibody recognizes an epitope on human, mouse, and rat PSA, which, in vertebrates, is found linked to the extracellular domain of the neural cell adhesion molecule (NCAM, CD56).” However, it must be clarified that it recognizes PSA on protein acceptors other than NCAM.

NCAM, neural cell adhesion molecule.

#### Increased apoptosis in GM-CSF cultured *Gata1*-KO<sup>DC</sup> DCs

The reduction in the splenic DC compartment in *Gata1*-KO<sup>DC</sup> mice could be caused by either a block in DC differentiation, aberrant migration from the spleen, or enhanced apoptosis. The intrinsic role of GATA1 in differentiation and survival has been well established in erythroid progenitor cells (26, 28–31). Furthermore, we previously showed that induced ubiquitous deletion of *Gata1* (ER-Cre under the *Rosa26* promoter) affects megakaryopoiesis and erythropoiesis (52), as well as DC survival, whereas M-CSF BM-derived macrophages are not affected by *Gata1* recombination (24). To examine whether DC-specific GATA1 loss in committed DCs would result in enhanced apoptosis and/or defective differentiation, BM cells from WT<sup>lox</sup> and *Gata1*-KO<sup>DC</sup> mice were cultured in the presence of GM-CSF to generate DCs. The GM-CSF BM culture system is widely used for DC studies. These GM-CSF-derived DCs do not resemble cDCs but an inflammatory DC type, and the cultures also support the differentiation of monocyte-derived macrophages to some extent (53). We characterized the cultures by flow cytometry using CD11b, CD11c, and MHC-II. The cultures were very homogeneous based on expression of these markers and contained <20% of macrophage-like cells based on lower CD11c and higher CD11b expression, or by using F4/80 as a macrophage marker (Fig. 2A, Supplemental Fig. 1D, 1E).

Cells were stimulated with LPS or left unstimulated at day 7 and harvested after 60 h for RNA extraction, protein isolation, and flow cytometry analysis. Both WT<sup>lox</sup> and *Gata1*-KO<sup>DC</sup> cultured DCs were equally activated as shown by increased expression of MHC-II and costimulatory molecules CD86 and CD40 (Fig. 2B). We found a 2-fold reduction of *Gata1* mRNA in *Gata1*-KO<sup>DC</sup> cultures in steady-state. WT<sup>lox</sup> DCs upregulated *Gata1* expression upon LPS stimulation, as previously described (23); however, *Gata1*-KO<sup>DC</sup> DCs failed to do so. These results were confirmed at the protein level, although to a lesser extent, probably because of the half-life of GATA1 protein (Supplemental Fig. 1B).

To study the cell survival of WT<sup>lox</sup> and *Gata1*-KO<sup>DC</sup> cultures, we used Annexin V and PI staining. *Gata1*-KO<sup>DC</sup> cells cultured for

8 d, and stimulated for 24 h with LPS, showed a small decrease in live cells (Annexin V and PI double-negative cells) and an increase in apoptotic cells (Annexin V and PI double-positive cells) in comparison with WT<sup>lox</sup> DC cultures (Fig. 2D). Analysis on day 10, that is, 60 h in the presence of LPS, showed that, although the cells were maintained in WT<sup>lox</sup> DC cultures, there was a clear reduction of live cells and a strong increase in the percentage of apoptotic and dead cells in *Gata1*-KO<sup>DC</sup> cultures (Fig. 2D).

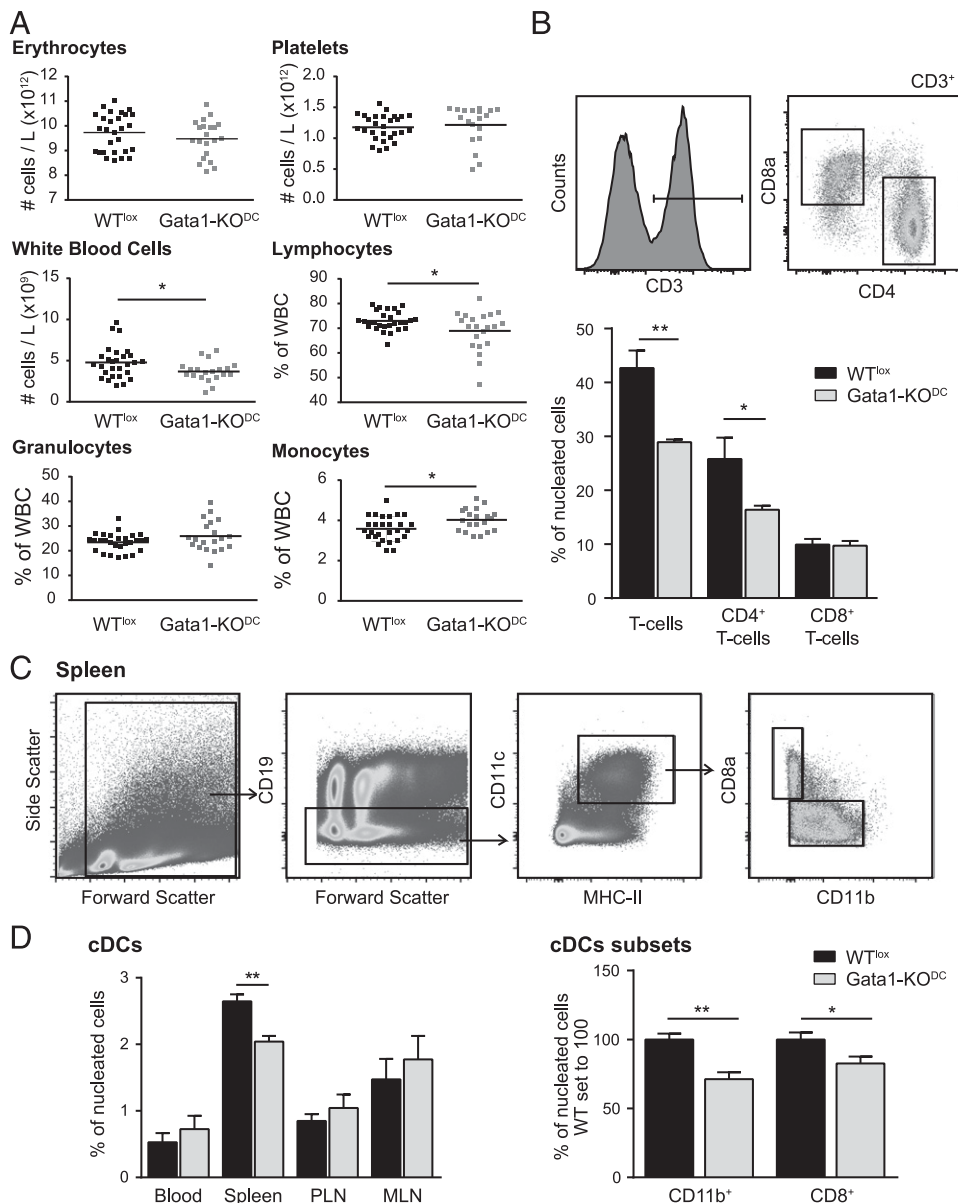
These results corroborate previous data (24) and highlight the requirement of *Gata1* in the regulation of the life span of differentiated and activated DCs.

#### RNA-Seq analysis of *Gata1*-KO<sup>DC</sup> DCs in steady-state and upon LPS stimulation

We next analyzed the changes in the transcriptome of *Gata1*-KO<sup>DC</sup> BM-DCs by RNA-Seq analysis. *Gata1*-KO<sup>DC</sup> mice were crossed with R26R-RG reporter mice (36), which express EGFP on the outer membrane and mCherry on the nuclear membrane upon recombination. BM-DCs from R26R-RG|WT<sup>Cre</sup> and R26R-RG|*Gata1*-KO<sup>DC</sup> mice were stimulated at day 7 and FACS-sorted for EGFP-mCherry double-positive cells 60 h thereafter (Fig. 3A), after which mRNA was extracted. This allowed us to enrich for DCs that underwent recombination, because *Gata1* levels were downregulated 8- to 18-fold in R26R-RG|*Gata1*-KO<sup>DC</sup> DCs compared with WT<sup>Cre</sup> (Fig. 3B). Furthermore, PCA of our data sets in comparison with publicly available RNA-Seq data sets of cultured GM-CSF DCs and G-CSF macrophages show that all DC data sets separate clearly from macrophages, corroborating the DC identity of our samples (Supplemental Fig. 1F).

RNA-Seq analysis revealed minor changes between R26R-RG|*Gata1*-KO<sup>DC</sup> and WT<sup>Cre</sup> DC in steady-state cultures, that is, 15 genes were significantly upregulated and 15 genes significantly downregulated. However, upon LPS stimulation, 289 genes were significantly upregulated and 609 genes were significantly downregulated in R26R-RG|*Gata1*-KO<sup>DC</sup> DCs compared with WT<sup>Cre</sup> (Fig. 3C, 3D, Supplemental Fig. 2B, Supplemental Table I). These results suggest

**FIGURE 1.** GATA1 loss in DCs results in a reduction of the splenic DC compartment. **(A)** Blood parameters of Gata1-KO<sup>DC</sup> and WT<sup>lox</sup> mice in the steady-state were determined using a Scil Vet abc Plus+ Hematology analyzer. Absolute numbers of erythrocytes, platelets, and WBCs were counted per liter. Further subdivision of lymphocytes, granulocytes, and monocytes are depicted as percentage of WBCs. **(B)** Flow cytometry analysis of the lymphocytes in the bloodstream. T cells were selected for CD3 expression and further subdivided into CD4<sup>+</sup> and CD8<sup>+</sup> T cells. **(C)** DC gating strategy from splenic tissue. First, all nucleated cells were selected, from which the non-B cells (CD19<sup>neg</sup> cells) were selected. Next, the CD11c<sup>+</sup> MHC-II<sup>+</sup> cells were selected as cDCs, which were further subdivided into CD8<sup>+</sup> or CD11b<sup>+</sup> subsets. **(D)** The percentage of DCs is shown in different tissues, depicted as percentage of all nucleated cells. Splenic cDCs were further subdivided into CD8<sup>+</sup> or CD11b<sup>+</sup> subsets, depicted as percentage of all nucleated cells, setting values obtained for WT<sup>lox</sup> animals to 100%. At least three independent experiments, each including three mice per genotype, were used for the analysis. \**p* ≤ 0.05, \*\**p* ≤ 0.01.



a major role for GATA1 in transcriptional regulation of DC upon activation.

HOMER transcription factor motif analysis revealed CEBP motif enrichment in the differentially expressed genes in steady-state conditions (Fig. 3C). Upon LPS stimulation, we identified ETS and CEBP motifs significantly enriched in the set of upregulated genes (Fig. 3D). Cooperation of CEBPα/ETS and GATA1 has been previously reported in eosinophils (54). A different set of enriched motifs was identified when taking downregulated genes, which included motifs for TAL1, bZIP, Maz (ZF), ETS, and TBP. Transcription factors recognizing these motifs have been reported to interact directly or to cooperate with GATA1 or other GATA transcription factors (55–64). GO term enrichment analyses revealed a number of specific processes that were affected in R26R-RG|Gata1-KO<sup>DC</sup> DCs upon LPS stimulation. An increased representation of metabolic processes was observed in the set of upregulated genes, and in the set of downregulated genes we observed migration, proliferation, and DC differentiation, but also T cell activation and CD4<sup>+</sup> T cell activation to be affected (Supplemental Table II).

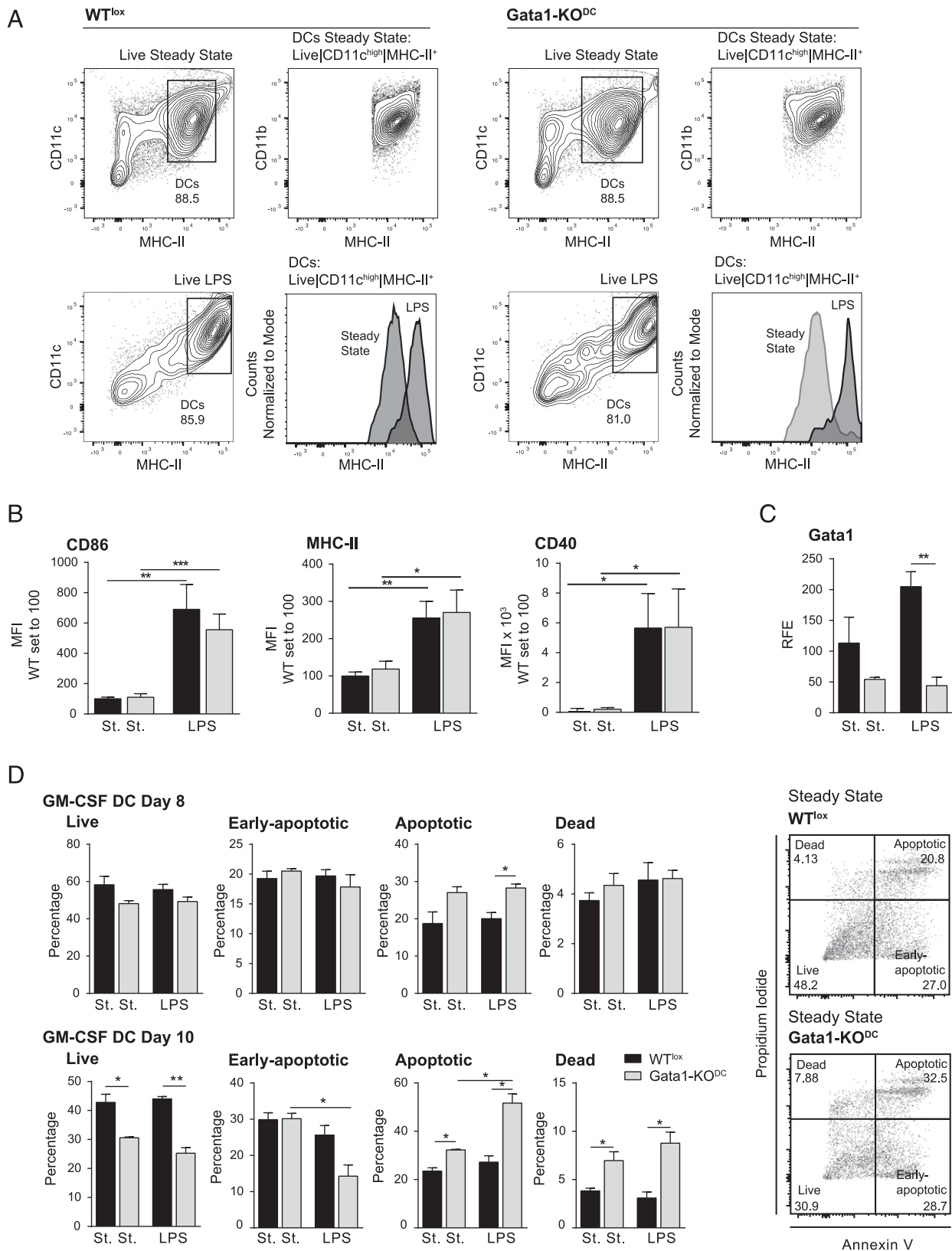
Ingenuity Pathway Analysis (IPA) allowed us to assign the differentially expressed genes into functional categories (Supplemental

Fig. 2A). Interestingly, we observed 58 transcriptional regulators that were affected upon LPS stimulation, of which 7 were upregulated and 51 were downregulated (Table II). These include *Gata2*, *Ikaros3* and *Ikaros4*, *Irf8*, *Nfkb*, *Bach2*, *Vdr*, *Runx1*, and *Runx3*, all with known roles in DC development and function, which could on their own explain the DC deficiency observed in steady-state conditions in vivo and the apoptosis observed in vitro. Not appearing in the IPA, but shown to be relevant for DC specification, *Zbtb46* (53, 65) was also downregulated significantly in Gata1-KO<sup>DC</sup> DCs upon LPS stimulation.

This finding together with the HOMER motif enrichment analysis, in which the GATA motif was not found to be enriched, supports the notion that transcriptional differences identified in R26R-RG|Gata1-KO<sup>DC</sup> DCs include many indirect GATA1 targets.

*DC migration toward the lymph nodes upon LPS stimulation is impaired in Gata1-KO<sup>DC</sup> mice*

The effect of Gata1 loss on the DC transcriptome was major in LPS-stimulated DCs, as shown by RNA-Seq analysis. Therefore, we studied the impact of DC-specific Gata1 loss in vivo in a sterile sepsis



**FIGURE 2.** Increased apoptosis in GM-CSF cultured Gata1-KO<sup>DC</sup> DCs. **(A)** Flow cytometry analysis of GM-CSF cultures of WT<sup>lox</sup> and Gata1-KO<sup>DC</sup> DCs in steady-state and upon LPS stimulation. DCs are gated as MHC-II<sup>high</sup> CD11c<sup>+</sup>. **(B)** Gated DCs were analyzed by flow cytometry for expression of the activation markers CD86, MHC-II, and CD40, which are depicted as mean fluorescence intensity (MFI). WT steady state (St. St.) is set to 100. **(C)** Relative expression of *Gata1* mRNA in GM-CSF cultured DCs. **(D)** Cultured DCs treated or left untreated with LPS at day 7 were harvested at day 8 or 10 of culture. Cells were stained for Annexin V and PI and analyzed by flow cytometry. Cells were gated for live cells (Annexin V<sup>neg</sup>, PI<sup>neg</sup>), early apoptotic cells (Annexin V<sup>+</sup>, PI<sup>neg</sup>), apoptotic cells (Annexin V<sup>+</sup>, PI<sup>+</sup>), or dead cells (Annexin V<sup>neg</sup>, PI<sup>+</sup>). Bar graphs depicting all four populations at both days are shown. Representative dot plots are shown on the right. \**p* ≤ 0.05, \*\**p* ≤ 0.01, \*\*\**p* ≤ 0.001. RFE, relative fold enrichment.



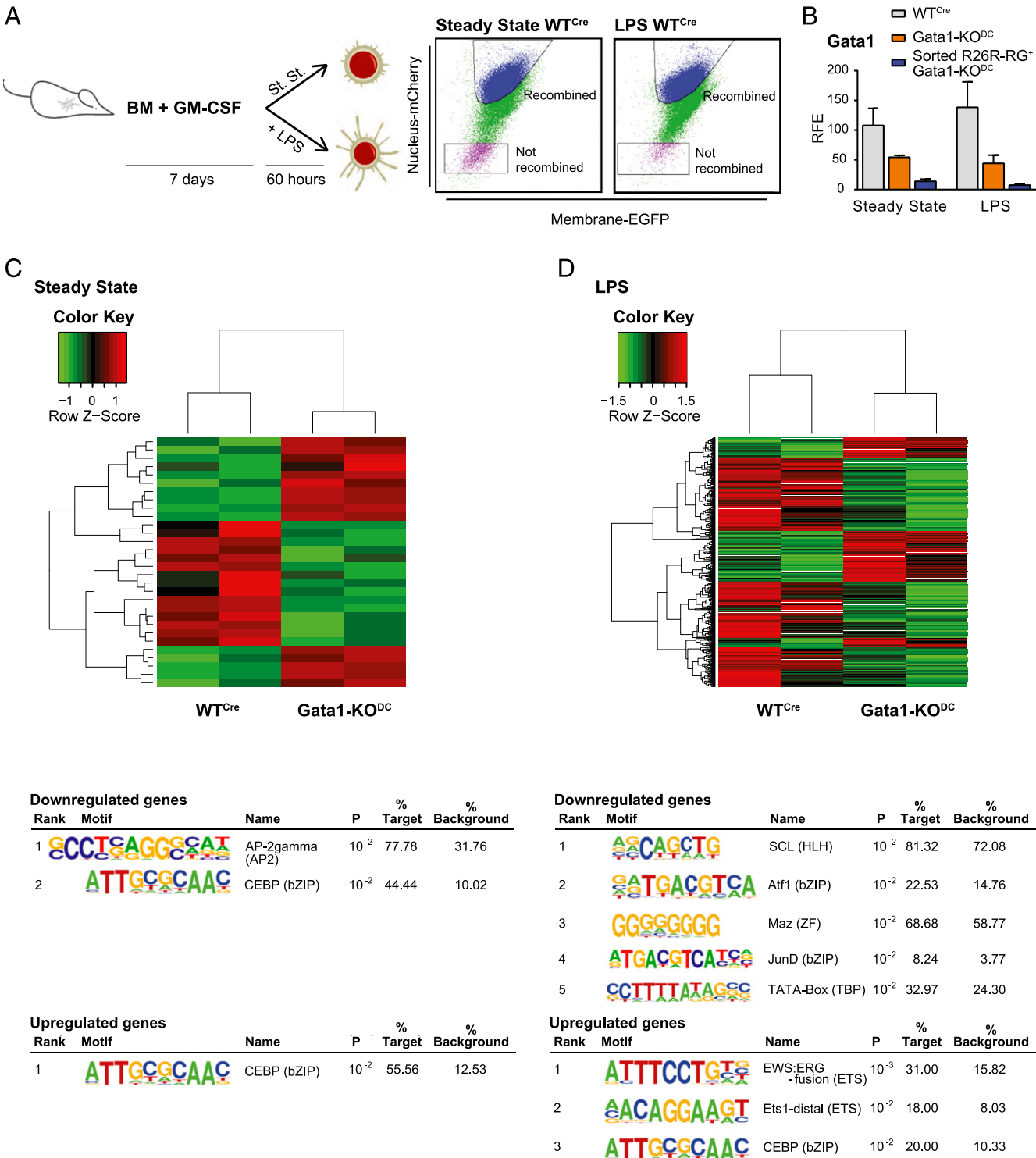


**FIGURE 3.** RNA-Seq analysis of *Gata1*-KO<sup>DC</sup> DCs in steady-state and upon LPS stimulation. **(A)** Graphic overview of the experiment. Mouse BM cells were cultured in the presence of GM-CSF. At day 7, half of the cells were stimulated with LPS, and the other half was left in steady-state condition (ST). At day 10, cells were harvested and sorted for RNA extraction. DCs from R26R-RG|WT<sup>Cre</sup> and R26R-RG|KO<sup>DC</sup> DC cultures were sorted for GFP<sup>+</sup>/mCherry<sup>+</sup> cells. Dot plots of the sorting strategy are shown. **(B)** quantitative RT-PCR analysis of *Gata1* expression levels are depicted for sorted GFP<sup>+</sup>/mCherry<sup>+</sup> WT<sup>Cre</sup> DCs, KO<sup>DC</sup> cultures (before sorting), and sorted R26R-RG|KO<sup>DC</sup> DCs. *Gata1* levels were further reduced in the sorted R26R-RG|KO<sup>DC</sup> cells, and these were used for RNA-Seq analysis. **(C)** Heat map (Z-scores) of significantly deregulated genes in R26R-RG|KO<sup>DC</sup> DCs in steady state, including HOMER motif enrichment analysis for downregulated and upregulated genes. **(D)** Heat map (Z-scores) of significantly deregulated genes in R26R-RG|KO<sup>DC</sup> DCs upon LPS stimulation, including HOMER motif enrichment analysis for downregulated and upregulated genes. \**p* ≤ 0.05, \*\**p* ≤ 0.01, \*\*\**p* ≤ 0.001. RFE, relative fold enrichment.

model, 24 h after i.v. injection of LPS into WT<sup>lox</sup> and *Gata1*-KO<sup>DC</sup> mice. After LPS treatment, both WT<sup>lox</sup> and *Gata1*-KO<sup>DC</sup> splenic DCs were significantly lower compared with PBS controls. Interestingly, we observed that, although LPS induces an increase in DC

numbers in the peripheral lymph nodes (PLNs) (e.g., axillary and inguinal lymph nodes) of WT<sup>lox</sup> mice, this increase was not observed in the PLNs from *Gata1*-KO<sup>DC</sup> mice (Fig. 4A). This might be because of increased apoptosis in *Gata1*-KO<sup>DC</sup> mice or reduced DC



Table II. IPA of transcriptional regulators

Symbol	Log Ratio	Entrez Gene Name/Description
Prdm8	-6.3770	PR domain containing 8
Ikzf3	-6.0240	IKAROS family zinc finger 3 (Aiolos)
Insm1	-5.7090	Insulinoma-associated 1
Nrarp	-5.1290	NOTCH-regulated ankyrin repeat protein
Myb	-4.4890	v-myb avian myeloblastosis viral oncogene homolog
Meis1	-4.0850	Meis homeobox 1
Pou4f1	-3.8220	POU class 4 homeobox 1
Bach2	-3.5780	BTB and CNC homology 1, basic leucine zipper transcription factor 2
Ptrf	-3.2420	Polymerase I and transcript release factor
Vdr	-3.1090	Vitamin D (1,25-dihydroxyvitamin D3) receptor
Zfp366	-3.0920	Zinc finger protein 366
Tcf7	-3.0860	Transcription factor 7, T cell specific
Stat4	-2.8500	Signal transducer and activator of transcription 4
Aff3	-2.7920	AF4/FMR2 family, member 3
Satb1	-2.7570	SATB homeobox 1
Sp6	-2.7230	Sp6 transcription factor
Cbfa2t3	-2.6880	Core-binding factor, runt domain, $\alpha$ subunit 2; translocated to, 3
Ssbp3	-2.5000	Single-stranded DNA binding protein 3
Zeb1	-2.4930	Zinc finger E-box binding homeobox 1
Jdp2	-2.4870	Jun dimerization protein 2
Kdm4a	-2.4290	Lysine (K)-specific demethylase 4A
Gata2	-2.4120	GATA binding protein 2
Irf8	-2.3680	IFN regulatory factor 8
Ncoa7	-2.2690	Nuclear receptor coactivator 7
Ikzf4	-2.2400	IKAROS family zinc finger 4 (Eos)
Hdac11	-2.1510	Histone deacetylase 11
Batf3	-2.1360	Basic leucine zipper transcription factor, ATF-like 3
Ciita	-2.1350	Class II, MHC, transactivator
Crem	-2.0510	cAMP responsive element modulator
Uhrf1	-2.0260	Ubiquitin-like with PHD and ring finger domains 1
Rel	-1.9660	v-rel avian reticuloendotheliosis viral oncogene homolog
Ezh2	-1.9430	Enhancer of zeste 2 polycomb repressive complex 2 subunit
Stat5a	-1.9260	Signal transducer and activator of transcription 5A
Phc1	-1.9140	Polyhomeotic homolog 1 (Drosophila)
Smarce1	-1.8770	SWI/SNF related
Aebp2	-1.7660	AE binding protein 2
Mkl1	-1.7020	Megakaryoblastic leukemia (translocation) 1
Tcf4	-1.6210	Transcription factor 4
Psmg4	-1.5950	Proteasome (prosome, macropain) assembly chaperone 4
Nfil3	-1.5780	NF, IL 3 regulated
Runx3	-1.5250	Runt-related transcription factor 3
Zbtb42	-1.5050	Zinc finger and BTB domain containing 42
Sp140	-1.4530	SP140 nuclear body protein
Tfdp2	-1.4530	Transcription factor Dp-2 (E2F dimerization partner 2)
Ets2	-1.4010	v-ets avian erythroblastosis virus E26 oncogene homolog 2
Hsf2	-1.3970	Heat shock transcription factor 2
Nfkb1	-1.3630	NF of $\kappa$ light polypeptide gene enhancer in B-cells 1
Foxp1	-1.3350	Forkhead box P1
Runx2	-1.2910	Runt-related transcription factor 2
Zkscan17	-1.2790	Zinc finger protein 496
Jazf1	-1.2380	JAZF zinc finger 1
Trim29	2.1090	Tripartite motif containing 29
Maged1	1.9030	Melanoma Ag family D, 1
Stl8	1.6580	Suppression of tumorigenicity 18, zinc finger
Creg1	1.5720	Cellular repressor of E1A-stimulated genes 1
Tanc2	1.3270	Tetratricopeptide repeat, ankyrin repeat and coiled-coil containing 2
Tfeb	1.3060	Transcription factor EB
Lmo4	1.2520	LIM domain only 4

LPS KO versus WT: transcriptional regulators of significant differentially expressed genes.

migration. As shown in Fig. 2E, there were slightly more apoptotic cells in the Gata1-KO<sup>DC</sup> DC cultures compared with WT<sup>lox</sup>, and no differences were observed in early apoptotic cells or dead cells 24 h upon LPS stimulation.

Therefore, we next studied whether the reduced number of DCs in the PLN could be caused by a reduction in migratory DCs. Based on MHC-II expression, we further categorized the DCs in the PLN into migratory DCs (CD11c<sup>+</sup>[MHC-II<sup>high</sup>]) and resident DCs (CD11c<sup>+</sup>[MHC-II<sup>mid</sup>]) and identified a reduction in migratory DCs (Fig. 4B). This indicates that GATA1-regulated genes are not only

involved in cell survival but also in migration of DCs after activation. This is in agreement with our RNA-Seq GO term enrichment analysis.

#### *Gata1-KO<sup>DC</sup> DCs display normal CCR7 expression but have impaired migration toward CCL21*

DC migration to the lymph nodes is dependent on the CCR7 (66), and upregulation of *Ccr7* is correlated with the activation of DCs. Furthermore, RNA-Seq analysis showed a reduction of mRNA expression of *Ccr7* in Gata1-KO<sup>DC</sup> DCs. We therefore cultured DCs

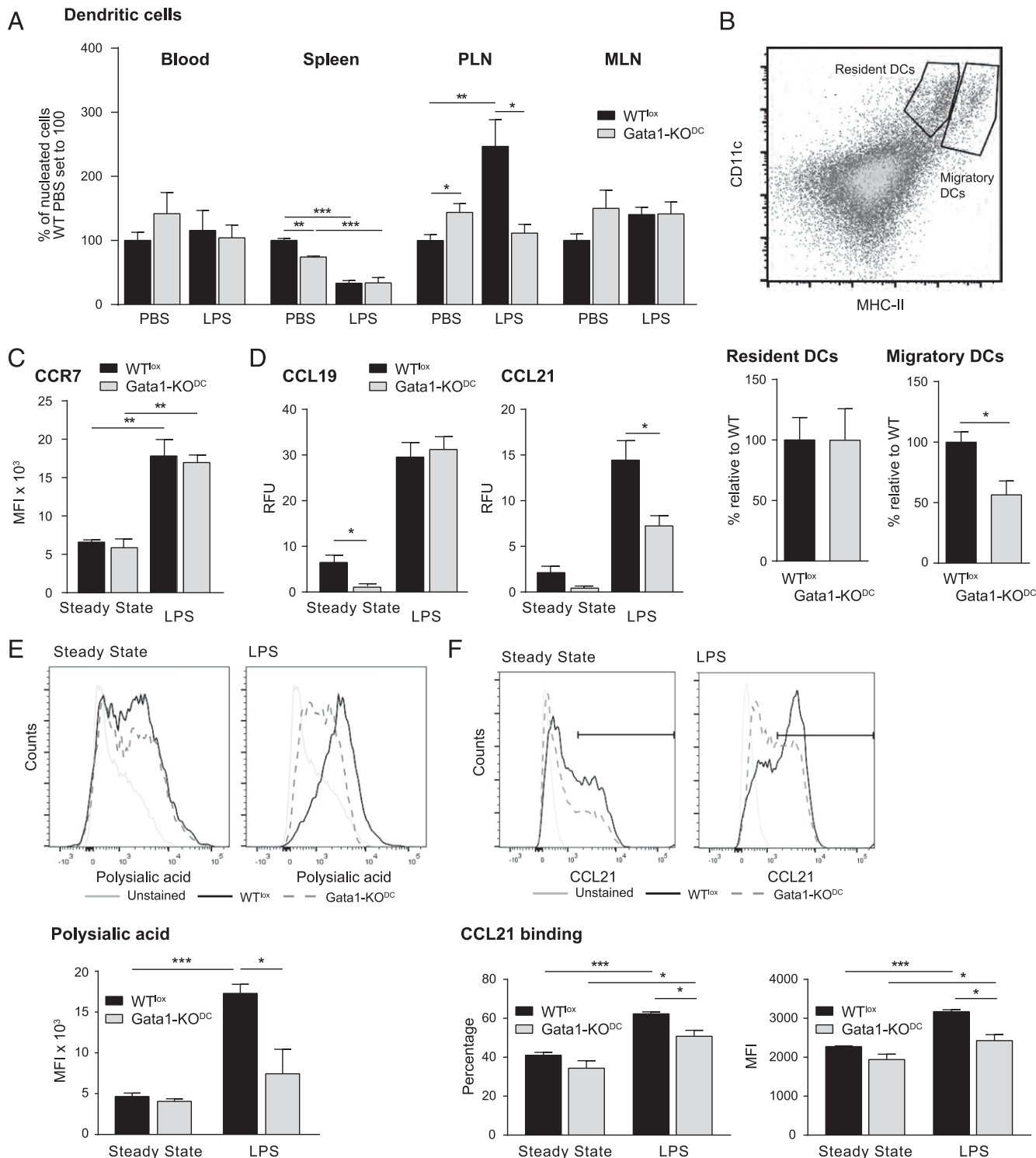


**FIGURE 4.** Impaired migration capacity of Gata1-KO<sup>DC</sup> DCs toward the lymph nodes is selective for CCL21. **(A)** Percentages of DCs in different tissues 24 h after PBS or LPS injection, depicted as percentage of all nucleated cells. Samples were normalized to WT-PBS. **(B)** DCs were subdivided in LN-resident DCs and migratory DCs based on MHC-II expression. **(C)** Expression of CCR7 on the surface of GM-CSF cultured DCs from WT<sup>lox</sup> or KO<sup>DC</sup> mice. **(D)** Migration of GM-CSF cultured DCs toward CCL19 or CCL21 expressed in relative fluorescence units (RFU). **(E)** Expression of PSA on the surface of GM-CSF cultured DCs from WT<sup>lox</sup> or Gata1-KO<sup>DC</sup> mice. **(F)** CCL21 binding assay. The percentage of cells binding CCL21 and the mean fluorescence intensity (MFI) of CCL21 binding are depicted in respective bar graphs. Representative histograms are shown.  $p \leq 0.05$ ,  $**p \leq 0.01$ ,  $***p \leq 0.001$ .

with GM-CSF and analyzed the expression of CCR7 upon LPS stimulation on the cell surface. Surprisingly, both WT<sup>lox</sup> and Gata1-KO<sup>DC</sup> DCs showed an equally strong upregulation of CCR7 after LPS stimulation (Fig. 4C). To gain insight in the migration defect observed in vivo, we performed in vitro migration assays using different chemoattractants.

We tested the response of WT<sup>lox</sup> and Gata1-KO<sup>DC</sup> BM-DCs toward CCL19 and CCL21, which are the only known ligands for CCR7 (67). As expected, steady-state DC migration toward CCL19 and CCL21 was minimal. Gata1-KO<sup>DC</sup> DCs appeared to be even less responsive than WT<sup>lox</sup> DCs, as corroborated by the random migration observed in the absence of chemoattractant

(Supplemental Fig. 1C). Upon LPS stimulation, DCs upregulate the CCR7 receptor and become responsive to CCL19 and CCL21. The migration toward CCL19 was increased in both WT<sup>lox</sup> and Gata1-KO<sup>DC</sup> DCs to similar levels. However, migration toward CCL21 was strongly impaired in Gata1-KO<sup>DC</sup> DCs (Fig. 4D).

CCL19 and CCL21 are very similar to each other; however, unlike CCL19, CCL21 contains a highly basic C-terminal tail that inhibits binding to CCR7 (68). After LPS stimulation, DCs highly upregulate PSA decoration of their surface proteins. PSA groups immobilize the tail of CCL21, thus enabling its binding to CCR7 (69, 70). Supporting this notion, it has been shown that enzymatic depletion of PSA affects migration toward CCL21, but not to CCL19 (68–70). We next measured PSA expression in our cultures and observed that, as expected, PSA expression was highly induced upon LPS activation on WT<sup>lox</sup> DCs. Although we observed some PSA induction in Gata1-KO<sup>DC</sup> DCs upon LPS activation, it was significantly lower than in WT<sup>lox</sup> DCs (Fig. 4E). To ensure that the decreased PSA levels indeed affected CCL21 binding, we performed a CCL21 binding assay. We found that the capacity of Gata1-KO<sup>DC</sup> DCs to bind CCL21 was significantly reduced, although moderately (Fig. 4F). These data explain the selective defective migration of Gata1-KO<sup>DC</sup> DCs toward CCL21, whereas leaving DC migration toward CCL19 intact. This is in agreement with the glycosylation-specific effects on ligand binding to CCR7

(68–70). Interestingly, the RNA-Seq data revealed that *St3Gal3*, a sialyltransferase, was significantly downregulated in Gata1-KO<sup>DC</sup> DCs upon LPS stimulation when compared with WT<sup>Cre</sup> DCs. A deficiency in sialic acid transfer further supports the lower surface expression of PSA displayed by Gata1-KO<sup>DC</sup> DCs upon LPS stimulation and the consequent reduction in CCL21 binding capacity (although moderate), which results in impaired (but not abolished) migration toward CCL21.

#### *Steady-state DC influx to lymph nodes is defective in aging Gata1-KO<sup>DC</sup> mice*

Adequate migration of DCs toward the lymph nodes is essential for maintaining the balance of the mounted immune response, and it is essential that the steady-state flux of DCs toward lymph nodes is kept in balance throughout life. Because we have observed defective migration of Gata1-KO<sup>DC</sup> DCs toward lymph nodes as a result of an acute response toward LPS stimulation, and we have identified that this defect is CCL21 selective, we hypothesized that the steady-state influx of DC migration toward lymph nodes would be impaired. To test this hypothesis, we allowed Gata1-KO<sup>DC</sup> mice and WT<sup>lox</sup> littermates to age, and sacrificed them to analyze the DC compartment at around 40 wk of age. We did not observe notable differences in organ sizes (data not shown), or in organ absolute cell numbers (Fig. 5C). Flow cytometry analysis of the DC

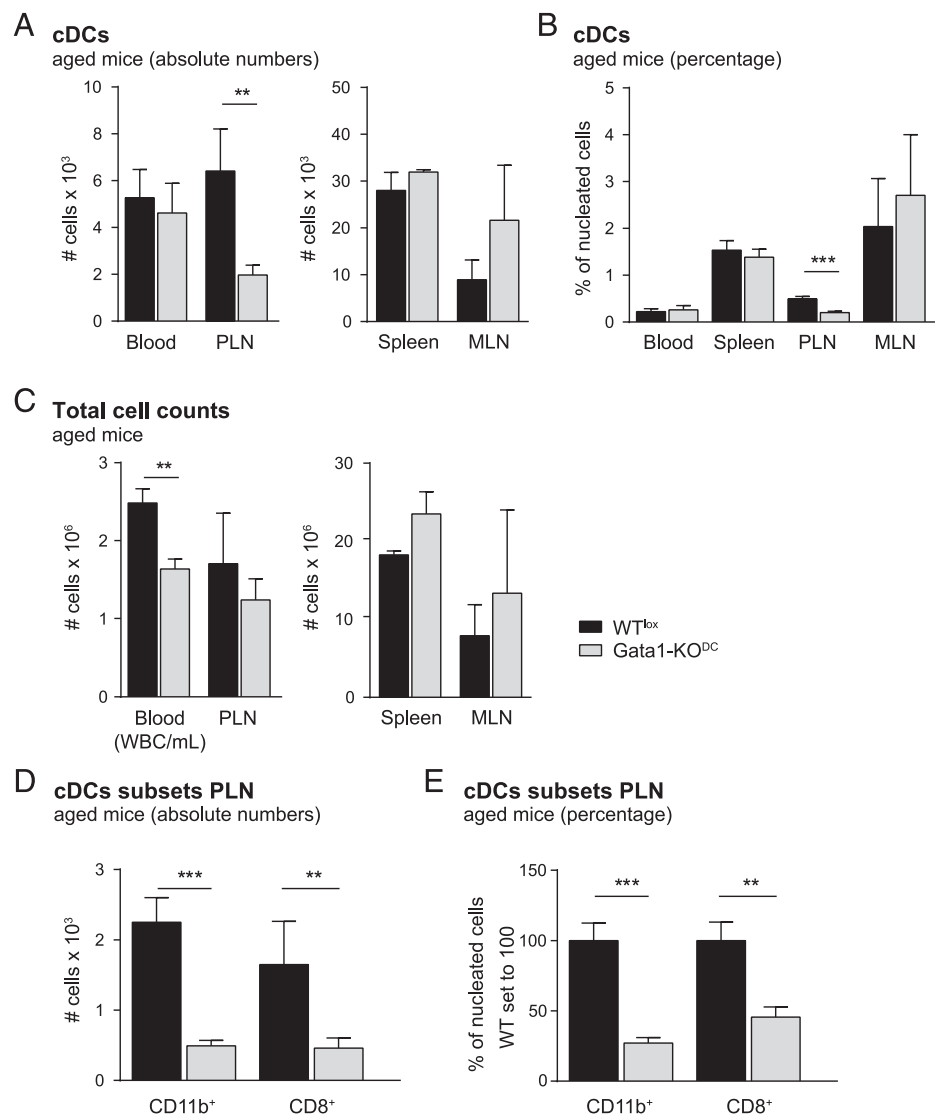


**FIGURE 5.** Defective steady-state influx of DCs toward lymph nodes as seen in aging Gata1-KO<sup>DC</sup> mice. **(A)** The absolute number of DCs found in different tissues of aged mice (around 40 wk of age). **(B)** The percentage of DCs in different tissues of aged mice, depicted as percentage of all nucleated cells. **(C)** Total number of cells isolated from different tissues of aged mice. **(D)** cDCs from PLNs were further subdivided into CD8<sup>+</sup> or CD11b<sup>+</sup> subsets. Absolute cell numbers were depicted. **(E)** CD8<sup>+</sup> or CD11b<sup>+</sup> subsets from the PLNs were depicted as percentage of all nucleated cells. Values obtained for WT<sup>lox</sup> animals are set to 100%. \*\**p* ≤ 0.01, \*\*\**p* ≤ 0.001.

compartment in the spleen revealed, in contrast with young mice, no significant differences in Gata1-KO<sup>DC</sup> versus WT<sup>lox</sup> aged mice both in percentage and absolute numbers. DCs were significantly reduced in lymph nodes of Gata1-KO<sup>DC</sup> aged mice compared with WT<sup>lox</sup> aged mice; this was not found in young mice (Fig. 5A, 5B, gating in Fig. 1C). Further subdivision into CD11b<sup>+</sup> and CD8<sup>+</sup> subsets revealed that the decrease of total cDCs in the PLN was due to a decrease in both subsets, with CD11b<sup>+</sup> DCs more strongly affected (Fig. 5D, 5E).

Taken together, GATA1 loss in DCs affects DC survival and migration capacity in homeostatic conditions and upon activation. We identified a selective impairment of Gata1-KO<sup>DC</sup> DCs to migrate toward CCL21, which could be explained by lower expression of PSA upon DC activation. In young mice, this defect is reflected by the initial DC reduction in spleen in homeostatic conditions, followed by impaired influx of DCs in lymph nodes upon sterile inflammation. In aged mice, we observe abnormal DC homeostasis in the PLNs, whereas the DC numbers in the spleen are within the normal range. The reason for this shift in DC homeostasis from spleen to PLN in aging mice might be because of the prolonged (or chronic) pressure of the net effect of migration and survival defects caused by GATA1 loss. However, no strong evidence for this is provided.

## Discussion

Transcription factor GATA1 is essential in the erythroid, eosinophilic, and megakaryocytic lineages (25–27, 29). It is also expressed in mast cells, although GATA1 is dispensable in this lineage (71). We previously reported that GATA1 is important for the development of murine DCs (24, 27). Similarly, the role of GATA1 during human DC differentiation from monocytes was reported by another group (26). In this study, we further dissected the role of GATA1 in DCs with the use of a DC-specific *Gata1* KO mouse model, a necessary step to understand the role of GATA1 in DCs because previous studies used inducible ubiquitous deletion of *Gata1*.

Gata1-KO<sup>DC</sup> mice displayed reduced numbers of DCs in the spleen in the steady-state. Because GATA1 is linked to the positive regulation of cell survival in several cell types (28, 30), we hypothesized this might also be a crucial function regulated by GATA1 in DCs. Indeed, we found increased apoptosis in cultured BM-derived Gata1-KO<sup>DC</sup> DCs.

RNA-Seq analysis of *Gata1* KO DCs compared with WT<sup>Cre</sup> DCs in the steady-state and upon LPS stimulation revealed major changes in the transcriptome in LPS-stimulated DCs, including deregulation of a plethora of other transcription regulators that are known to be essential in the DC lineage. GO term enrichment analysis revealed pathways related to cell survival, cell migration, and DC function. This led us to investigate the DC compartment in vivo upon induction of sterile inflammation by i.v. injection of LPS.

Interestingly, when we challenged the mice with LPS, we found a migration defect of Gata1-KO<sup>DC</sup> DCs toward the PLNs. DC migration toward the PLN is dependent on CCR7 receptor expression, which is strongly upregulated on the DC surface after activation (66, 72, 73). DCs deficient for CCR7 expression are not able to migrate to the lymph nodes (66, 72, 73). The expression of CCR7 is typically correlated to upregulation of DC activation markers (e.g., MHC-II, CD86, and CD40) but can also be induced in an activation-independent manner, for example, after uptake of apoptotic cells (72). CCR7 protein expression on the surface of Gata1-KO<sup>DC</sup> DCs was normal compared with WT<sup>lox</sup> DCs as shown by flow cytometry analysis. This suggested that there must be another mechanism interfering with the proper migration of Gata1-KO<sup>DC</sup> DCs toward the PLNs.

Because CCL19 and CCL21 are the known ligands for CCR7 receptor (67), we assayed in vitro the migration capacity of Gata1-KO<sup>DC</sup> DCs toward these chemoattractants. Steady-state DC migration toward CCL19 and CCL21 was as expected minimal, with Gata1-KO<sup>DC</sup> DCs apparently even less responsive than WT<sup>lox</sup> DCs, as corroborated by the random migration observed in the absence of chemoattractant. GO-Term analysis of our RNA-Seq data revealed alterations in “motility pathways.” One of the genes important for migration is myosin L chain kinase, and it is 4.1-fold downregulated in Gata1-KO<sup>DC</sup> DCs RNA-seq, which might explain this reduced motility. When we stimulated DCs with LPS, we observed a specific migration defect of Gata1-KO<sup>DC</sup> DCs toward CCL21. The two ligands are highly similar; however, unlike CCL19, CCL21 contains a highly basic C-terminal tail of 32 aa (67, 68). This C-terminal tail of CCL21 autoinhibits binding to CCR7 (69). PSA, highly expressed on activated DCs, fixes the C-terminal tail of CCL21, thereby facilitating its binding to CCR7 (69, 70). Depletion of PSA from the cell surface by Endo-neuraminidase treatment or small interfering RNA against St8sia4 sialyltransferase impairs migration toward CCL21, but not toward CCL19 (68–70). Indeed, we found a reduced expression of PSA on the surface of Gata1-KO<sup>DC</sup> DCs that could explain the defective migration toward CCL21, whereas retaining normal migration toward CCL19. Notably, the reduction of PSA surface levels in GATA1-KO<sup>DC</sup> DCs had only a moderate reduction effect on CCL21 binding. This suggests that there might be other determinants regulating CCL21 binding and selective DC migration, and we cannot exclude that they behave differently between Gata1-KO<sup>DC</sup> and WT DCs. Such determinants might include a potential transient character of the interaction between PSA and the CCL21 tail, receptor trafficking and downstream signaling (74), autocrine DC mechanisms that block DC cell migration (and potentially CCL21 binding), or DC survival (75, 76). CCL21, and not CCL19, was found to be the critical factor for DC homing to lymph nodes (77). The fact that proper DC migration toward CCL21 is dependent on the PSA surface levels led several groups to identify the receptors that need to be polysialylated to allow CCL21 to be recognized by CCR7. It has been suggested that PSA acceptor molecule Neuropilin-2 is the relevant factor involved in this process (see Rey-Gallardo et al. [68]), although downregulation in human monocyte-derived DCs did not completely abrogate the capacity to migrate toward CCL21. Recently, it has been shown that CCR7 itself carries PSA modifications (78); however, we do not know at what extent PSA downregulation affects either of the two PSA acceptors in Gata1-KO<sup>DC</sup> DCs compared with WT. Our study shows that proper sialylation depends on transcriptional programs, in particular downstream of GATA1, which are induced upon DC activation (i.e., LPS stimulation). Defects in this regulatory process lead to defective migration of DCs toward lymph nodes, not only upon an acute stimulus (i.e., LPS stimulation in vitro or in vivo) but also affecting the steady-state influx of DCs toward lymph nodes, as shown by the reduced number of DCs in lymph nodes in aging Gata1-KO<sup>DC</sup> mice.

PSA is a sugar molecule expressed on the cell surface of eukaryotic cells, with a complex biosynthesis involving multiple sialyltransferases (79). For example, a group of sialyltransferases adds sialic acid with an  $\alpha$ -2,3 linkage to galactose (i.e., St3gal sialyltransferases, including St3gal3, which uses *O*-glycans as well as *N*-glycans as substrate), whereas other sialyltransferases add sialic acid with an  $\alpha$ -2,6 linkage to galactose or *N*-acetylglucosamine (i.e., St6gal and St6galnac sialyltransferases including St6gal1, which uses *N*-glycans as substrate). A peculiar type of sialyltransferase adds sialic acid to other sialic acid units with an  $\alpha$ -2,8 linkage, forming structures referred to as PSA (i.e., St8sia sialyltransferases including St8sia4, which uses *N*-glycans as substrate) (80). Mice deficient for



St8sia4 completely lose PSA on the surface of DCs (81). RNA-Seq analysis revealed a number of sialyltransferases to be downregulated in Gata1-KO<sup>DC</sup> DCs, although only St3gal3 reached statistical significance. St3gal3 is not directly involved in PSA modification; however, it is involved in the generation of carbohydrate Ag sialyl-Lewis. As opposed to models in which St8sia4 is depleted, in our mice, PSA upregulation was partially abrogated, yet this is sufficient to negatively influence proper DC migration toward lymph nodes. Mice deficient for St3gal3 are more sensitive to allergic eosinophilic airway inflammation, indicating an important role of St3gal3 in the immune response (82), although the phenotype was explained as the result of lower Lewis group presence in the lung epithelium. However, the impact of loss of St3gal3 on DC polysialylation or migration has not been studied so far. Because the biosynthesis and transfer of PSA groups is a complex process, we suggest that the combinatorial deregulation of multiple sialyltransferases underlies reduced PSA surface expression of Gata1-KO<sup>DC</sup> DCs upon activation. The notion that low-abundance transcription factors such as GATA1 influence the fine-tuning of such relevant processes for proper DC function is of importance, because their manipulation might open new possibilities for the improvement of DC-based immunotherapy by targeting specific transcriptional programs.

## Disclosures

The authors have no financial conflicts of interest.

## References

- Naik, S. H. 2010. Generation of large numbers of pro-DCs and pre-DCs in vitro. *Methods Mol. Biol.* 595: 177–186.
- Shortman, K., and S. H. Naik. 2007. Steady-state and inflammatory dendritic cell development. *Nat. Rev. Immunol.* 7: 19–30.
- Dudziak, D., A. O. Kamphorst, G. F. Heidkamp, V. R. Buchholz, C. Trumpfheller, S. Yamazaki, C. Cheong, K. Liu, H. W. Lee, C. G. Park, et al. 2007. Differential antigen processing by dendritic cell subsets in vivo. *Science* 315: 107–111.
- Lahoud, M. H., A. I. Proietto, K. H. Gartlan, S. Kitsoulis, J. Curtis, J. Wettenhall, M. Sofi, C. Daunt, M. O'keeffe, I. Caminschi, et al. 2006. Signal regulatory protein molecules are differentially expressed by CD8<sup>+</sup> dendritic cells. *J. Immunol.* 177: 372–382.
- Liu, K., and M. C. Nussenzweig. 2010. Origin and development of dendritic cells. *Immunol. Rev.* 234: 45–54.
- Vremec, D., J. Pooley, H. Hochrein, L. Wu, and K. Shortman. 2000. CD4 and CD8 expression by dendritic cell subtypes in mouse thymus and spleen. *J. Immunol.* 164: 2978–2986.
- Schlitzer, A., N. McGovern, and F. Ginhoux. 2015. Dendritic cells and monocyte-derived cells: two complementary and integrated functional systems. *Semin. Cell Dev. Biol.* 41: 9–22.
- Dörner, B. G., M. B. Dörner, X. Zhou, C. Opitz, A. Mora, S. Güttler, A. Hutloff, H. W. Mages, K. Ranke, M. Schaefer, et al. 2009. Selective expression of the chemokine receptor CXCR1 on cross-presenting dendritic cells determines cooperation with CD8<sup>+</sup> T cells. *Immunity* 31: 823–833.
- Villadangos, J. A., and P. Schnorrer. 2007. Intrinsic and cooperative antigen-presenting functions of dendritic-cell subsets in vivo. *Nat. Rev. Immunol.* 7: 543–555.
- den Haan, J. M., and M. J. Bevan. 2002. Constitutive versus activation-dependent cross-presentation of immune complexes by CD8<sup>+</sup> and CD8<sup>−</sup> dendritic cells in vivo. *J. Exp. Med.* 196: 817–827.
- den Haan, J. M., S. M. Lehar, and M. J. Bevan. 2000. CD8<sup>+</sup> but not CD8<sup>−</sup> dendritic cells cross-prime cytotoxic T cells in vivo. *J. Exp. Med.* 192: 1685–1696.
- Belz, G. T., and S. L. Nutt. 2012. Transcriptional programming of the dendritic cell network. *Nat. Rev. Immunol.* 12: 101–113.
- Murphy, K. M. 2013. Transcriptional control of dendritic cell development. *Adv. Immunol.* 120: 239–267.
- Geissmann, F., M. G. Manz, S. Jung, M. H. Sieweke, M. Merad, and K. Ley. 2010. Development of monocytes, macrophages, and dendritic cells. *Science* 327: 656–661.
- Ichikawa, E., S. Hida, Y. Omatsu, S. Shimoyama, K. Takahara, S. Miyagawa, K. Inaba, and S. Taki. 2004. Defective development of splenic and epidermal CD4<sup>+</sup> dendritic cells in mice deficient for IFN regulatory factor-2. *Proc. Natl. Acad. Sci. USA* 101: 3909–3914.
- Suzuki, S., K. Honma, T. Matsuyama, K. Suzuki, K. Toriyama, I. Akitoyo, K. Yamamoto, T. Suematsu, M. Nakamura, K. Yui, and A. Kumatori. 2004. Critical roles of interferon regulatory factor 4 in CD11bhighCD8α<sup>+</sup> dendritic cell development. *Proc. Natl. Acad. Sci. USA* 101: 8981–8986.
- Wu, L., A. D'Amico, K. D. Winkel, M. Suter, D. Lo, and K. Shortman. 1998. RelB is essential for the development of myeloid-related CD8α<sup>+</sup> dendritic cells but not of lymphoid-related CD8α<sup>+</sup> dendritic cells. *Immunity* 9: 839–847.
- Tussiwand, R., B. Everts, G. E. Grajales-Reyes, N. M. Kretzer, A. Iwata, J. Bagaitkar, X. Wu, R. Wong, D. A. Anderson, T. L. Murphy, et al. 2015. Klf4 expression in conventional dendritic cells is required for T helper 2 cell responses. *Immunity* 42: 916–928.
- Hildner, K., B. T. Edelson, W. E. Purtha, M. Diamond, H. Matsushita, M. Kohyama, B. Calderon, B. U. Schraml, E. R. Unanue, M. S. Diamond, et al. 2008. Batf3 deficiency reveals a critical role for CD8α<sup>+</sup> dendritic cells in cytotoxic T cell immunity. *Science* 322: 1097–1100.
- Tamura, T., P. Taylor, K. Yamaoka, H. J. Kong, H. Tsujimura, J. J. O'Shea, H. Singh, and K. Ozato. 2005. IFN regulatory factor-4 and -8 govern dendritic cell subset development and their functional diversity. *J. Immunol.* 174: 2573–2581.
- Carotta, S., A. Dakic, A. D'Amico, S. H. Pang, K. T. Greig, S. L. Nutt, and L. Wu. 2010. The transcription factor PU.1 controls dendritic cell development and Flt3 cytokine receptor expression in a dose-dependent manner. *Immunity* 32: 628–641.
- Nutt, S. L., D. Metcalf, A. D'Amico, M. Polli, and L. Wu. 2005. Dynamic regulation of PU.1 expression in multipotent hematopoietic progenitors. *J. Exp. Med.* 201: 221–231.
- Scheenstra, M. R., V. Salunkhe, I. M. De Cuyper, M. Hoogenboezem, E. Li, T. W. Kuijpers, T. K. van den Berg, and L. Gutiérrez. 2015. Characterization of hematopoietic GATA transcription factor expression in mouse and human dendritic cells. *Blood Cells Mol. Dis.* 55: 293–303.
- Gutiérrez, L., T. Nikolic, T. B. van Dijk, H. Hammad, N. Vos, M. Willart, F. Grosveld, S. Philipsen, and B. N. Lambrecht. 2007. Gata1 regulates dendritic cell development and survival. *Blood* 110: 1933–1941.
- Kaneko, H., R. Shimizu, and M. Yamamoto. 2010. GATA factor switching during erythroid differentiation. *Curr. Opin. Hematol.* 17: 163–168.
- Göbel, F., S. Taschner, J. Jurkin, S. Konradi, C. Vaculik, S. Richter, D. Kneidinger, C. Mühlbacher, C. Bieglmayer, A. Elbe-Bürger, and H. Strobl. 2009. Reciprocal role of GATA-1 and vitamin D receptor in human myeloid dendritic cell differentiation. *Blood* 114: 3813–3821.
- Kozma, G. T., F. Martelli, M. Verrucci, L. Gutierrez, G. Migliaccio, M. Sanchez, E. Alfani, S. Philipsen, and A. R. Migliaccio. 2010. Dynamic regulation of Gata1 expression during the maturation of conventional dendritic cells. *Exp. Hematol.* 38: 489–503.e1.
- Caldwell, J. T., H. Edwards, A. A. Dombkowski, S. A. Buck, L. H. Matherly, Y. Ge, and J. W. Taub. 2013. Overexpression of GATA1 confers resistance to chemotherapy in acute megakaryocytic leukemia. *PLoS One* 8: e68601.
- Pevny, L., C. S. Lin, V. D'Agati, M. C. Simon, S. H. Orkin, and F. Costantini. 1995. Development of hematopoietic cells lacking transcription factor GATA-1. *Development* 121: 163–172.
- Tanaka, H., I. Matsumura, K. Nakajima, H. Daino, J. Sonoyama, H. Yoshida, K. Oritani, T. Machii, M. Yamamoto, T. Hirano, and Y. Kanakura. 2000. GATA-1 blocks IL-6-induced macrophage differentiation and apoptosis through the sustained expression of cyclin D1 and bcl-2 in a murine myeloid cell line M1. *Blood* 95: 1264–1273.
- Whyatt, D. J., A. Karis, I. C. Harkes, A. Verkerk, N. Gillemans, A. G. Elefanti, G. Vairo, R. Ploemacher, F. Grosveld, and S. Philipsen. 1997. The level of the tissue-specific factor GATA-1 affects the cell-cycle machinery. *Genes Funct.* 1: 11–24.
- Dickinson, R. E., H. Griffin, V. Bigley, L. N. Reynard, R. Hussain, M. Haniffa, J. H. Lakey, T. Rahman, X. N. Wang, N. McGovern, et al. 2011. Exome sequencing identifies GATA-2 mutation as the cause of dendritic cell, monocyte, B and NK lymphoid deficiency. *Blood* 118: 2656–2658.
- Onodera, K., T. Fujiwara, Y. Onishi, A. Itoh-Nakadai, Y. Okitsu, N. Fukuhara, K. Ishizawa, R. Shimizu, M. Yamamoto, and H. Harigae. 2016. GATA2 regulates dendritic cell differentiation. *Blood* 128: 508–518.
- Lindeboom, F., N. Gillemans, A. Karis, M. Jaegle, D. Meijer, F. Grosveld, and S. Philipsen. 2003. A tissue-specific knockout reveals that Gata1 is not essential for Sertoli cell function in the mouse. *Nucleic Acids Res.* 31: 5405–5412.
- Caton, M. L., M. R. Smith-Raska, and B. Reizis. 2007. Notch-RBP-J signaling controls the homeostasis of CD8<sup>+</sup> dendritic cells in the spleen. *J. Exp. Med.* 204: 1653–1664.
- Shioi, G., H. Kiyonari, T. Abe, K. Nakao, T. Fujimori, C. W. Jang, C. C. Huang, H. Akiyama, R. R. Behringer, and S. Aizawa. 2011. A mouse reporter line to conditionally mark nuclei and cell membranes for in vivo live-imaging. *Genesis* 49: 570–578.
- Brouwer, R. W., M. C. van den Hout, F. G. Grosveld, and W. F. van Ijcken. 2012. NARWHAL, a primary analysis pipeline for NGS data. *Bioinformatics* 28: 284–285.
- Kim, D., G. Pertea, C. Trapnell, H. Pimentel, R. Kelley, and S. L. Salzberg. 2013. TopHat2: accurate alignment of transcriptomes in the presence of insertions, deletions and gene fusions. *Genome Biol.* 14: R36.
- Flicek, P., M. R. Amodé, D. Barrell, K. Beal, K. Billis, S. Brent, D. Carvalho-Silva, P. Clapham, G. Coates, S. Fitzgerald, et al. 2014. Ensembl 2014. *Nucleic Acids Res.* 42: D749–D755.
- Liao, Y., G. K. Smyth, and W. Shi. 2013. The Subread aligner: fast, accurate and scalable read mapping by seed-and-vote. *Nucleic Acids Res.* 41: e108.
- Robinson, M. D., D. J. McCarthy, and G. K. Smyth. 2010. edgeR: a Bioconductor package for differential expression analysis of digital gene expression data. *Bioinformatics* 26: 139–140.
- Nota, B., J. D. Ndika, J. M. van de Kamp, W. A. Kanhai, S. J. van Dooren, M. A. van de Wiel, G. Pals, and G. S. Salomons. 2014. RNA sequencing of creatine transporter (SLC6A8) deficient fibroblasts reveals impairment of the extracellular matrix. *Hum. Mutat.* 35: 1128–1135.

43. Benjamini, Y., and Y. Hochberg. 1995. Controlling the false discovery rate: a practical and powerful approach to multiple testing. *J. R. Stat. Soc. Series B Stat. Methodol.* 57: 289–300.
44. Young, M. D., M. J. Wakefield, G. K. Smyth, and A. Oshlack. 2010. Gene ontology analysis for RNA-seq: accounting for selection bias. *Genome Biol.* 11: R14.
45. Heinz, S., C. Benner, N. Spann, E. Bertolino, Y. C. Lin, P. Laslo, J. X. Cheng, C. Murre, H. Singh, and C. K. Glass. 2010. Simple combinations of lineage-determining transcription factors prime cis-regulatory elements required for macrophage and B cell identities. *Mol. Cell* 38: 576–589.
46. Andrews, S. 2010. FastQC: A quality control tool for high throughput sequence data. Available at: <http://www.bioinformatics.babraham.ac.uk/projects/fastqc>. Accessed: June 10, 2016.
47. Bolger, A. M., M. Lohse, and B. Usadel. 2014. Trimmomatic: a flexible trimmer for Illumina sequence data. *Bioinformatics* 30: 2114–2120.
48. Li, H., B. Handsaker, A. Wysoker, T. Fennell, J. Ruan, N. Homer, G. Marth, G. Abecasis, and R. Durbin, 1000 Genome Project Data Processing Subgroup. 2009. The Sequence Alignment/Map format and SAMtools. *Bioinformatics* 25: 2078–2079.
49. Anders, S., P. T. Pyl, and W. Huber. 2015. HTSeq—a Python framework to work with high-throughput sequencing data. *Bioinformatics* 31: 166–169.
50. Leek, J. T., W. E. Johnson, H. S. Parker, A. E. Jaffe, and J. D. Storey. 2012. The sva package for removing batch effects and other unwanted variation in high-throughput experiments. *Bioinformatics* 28: 882–883.
51. Schmittgen, T. D., and K. J. Livak. 2008. Analyzing real-time PCR data by the comparative C(T) method. *Nat. Protoc.* 3: 1101–1108.
52. Gutiérrez, L., S. Tsukamoto, M. Suzuki, H. Yamamoto-Mukai, M. Yamamoto, S. Philipsen, and K. Ohneda. 2008. Ablation of Gata1 in adult mice results in aplastic crisis, revealing its essential role in steady-state and stress erythropoiesis. *Blood* 111: 4375–4385.
53. Helft, J., J. Böttcher, P. Chakravarty, S. Zelenay, J. Huotari, B. U. Schraml, D. Goubau, and C. Reis e Sousa. 2015. GM-CSF mouse bone marrow cultures comprise a heterogeneous population of CD11c(+)MHCII(+) macrophages and dendritic cells. *Immunity* 42: 1197–1211.
54. McNagny, K. M., M. H. Sieweke, G. Döderlein, T. Graf, and C. Nerlov. 1998. Regulation of eosinophil-specific gene expression by a C/EBP-Ets complex and GATA-1. *EMBO J.* 17: 3669–3680.
55. Antoniou, M., E. de Boer, E. Spanopoulou, A. Imam, and F. Grosveld. 1995. TBP binding and the rate of transcription initiation from the human beta-globin gene. *Nucleic Acids Res.* 23: 3473–3480.
56. Boopathi, E., J. A. Hypolite, S. A. Zderic, C. M. Gomes, B. Malkowicz, H. C. Liou, A. J. Wein, and S. Chacko. 2013. GATA-6 and NF- $\kappa$ B activate CPI-17 gene transcription and regulate Ca<sup>2+</sup> sensitization of smooth muscle contraction. *Mol. Cell. Biol.* 33: 1085–1102.
57. Georges, R., G. Nemer, M. Morin, C. Lefebvre, and M. Nemer. 2008. Distinct expression and function of alternatively spliced Tbx5 isoforms in cell growth and differentiation. *Mol. Cell. Biol.* 28: 4052–4067.
58. Gupta, V., A. A. Khan, B. K. Sasi, and N. R. Mahapatra. 2015. Molecular mechanism of monoamine oxidase A gene regulation under inflammation and ischemia-like conditions: key roles of the transcription factors GATA2, Sp1 and TBP. *J. Neurochem.* 134: 21–38.
59. Papadopoulos, P., L. Gutiérrez, J. Demmers, E. Scheer, F. Pourfarzad, D. N. Papageorgiou, E. Karkoulia, J. Strouboulis, H. J. van de Werken, R. van der Linden, et al. 2015. TAF10 interacts with the GATA1 transcription factor and controls mouse erythropoiesis. *Mol. Cell. Biol.* 35: 2103–2118.
60. Rodriguez, P., E. Bonte, J. Krijgsveld, K. E. Kolodziej, B. Guyot, A. J. Heck, P. Vyas, E. de Boer, F. Grosveld, and J. Strouboulis. 2005. GATA-1 forms distinct activating and repressive complexes in erythroid cells. *EMBO J.* 24: 2354–2366.
61. Simon, M. P., R. Tournaire, and J. Pouyssegur. 2008. The angiopoietin-2 gene of endothelial cells is up-regulated in hypoxia by a HIF binding site located in its first intron and by the central factors GATA-2 and Ets-1. *J. Cell. Physiol.* 217: 809–818.
62. Tallack, M. R., and A. C. Perkins. 2010. KLF1 directly coordinates almost all aspects of terminal erythroid differentiation. *IUBMB Life* 62: 886–890.
63. Tijssen, M. R., A. Cvejic, A. Joshi, R. L. Hannah, R. Ferreira, A. Forrai, D. C. Bellissimo, S. H. Oram, P. A. Smethurst, N. K. Wilson, et al. 2011. Genome-wide analysis of simultaneous GATA1/2, RUNX1, FLI1, and SCL binding in megakaryocytes identifies hematopoietic regulators. *Dev. Cell* 20: 597–609.
64. Toropainen, S., M. Malinen, S. Kaikkonen, M. Rytinki, T. Jääskeläinen, B. Sahu, O. A. Jänne, and J. J. Palvimäki. 2015. SUMO ligase PIAS1 functions as a target gene selective androgen receptor coregulator on prostate cancer cell chromatin. *Nucleic Acids Res.* 43: 848–861.
65. Satpathy, A. T., W. Kc, J. C. Albring, B. T. Edelson, N. M. Kretzer, D. Bhattacharya, T. L. Murphy, and K. M. Murphy. 2012. Zbtb46 expression distinguishes classical dendritic cells and their committed progenitors from other immune lineages. *J. Exp. Med.* 209: 1135–1152.
66. Ohl, L., M. Mohaupt, N. Czeloth, G. Hintzen, Z. Kiafard, J. Zwirner, T. Blankenstein, G. Henning, and R. Förster. 2004. CCR7 governs skin dendritic cell migration under inflammatory and steady-state conditions. *Immunity* 21: 279–288.
67. Förster, R., A. C. Davalos-Misslitz, and A. Rot. 2008. CCR7 and its ligands: balancing immunity and tolerance. *Nat. Rev. Immunol.* 8: 362–371.
68. Rey-Gallardo, A., C. Escribano, C. Delgado-Martín, J. L. Rodríguez-Fernández, R. Gerardy-Schahn, U. Rutishauser, A. L. Corbi, and M. A. Vega. 2010. Polysialylated neuropilin-2 enhances human dendritic cell migration through the basic C-terminal region of CCL21. *Glycobiology* 20: 1139–1146.
69. Bax, M., S. J. van Vliet, M. Litjens, J. J. García-Vallejo, and Y. van Kooyk. 2009. Interaction of polysialic acid with CCL21 regulates the migratory capacity of human dendritic cells. *PLoS One* 4: e6987.
70. Rey-Gallardo, A., C. Delgado-Martín, R. Gerardy-Schahn, J. L. Rodríguez-Fernández, and M. A. Vega. 2011. Polysialic acid is required for neuropilin-2 $\alpha$ /b-mediated control of CCL21-driven chemotaxis of mature dendritic cells and for their migration in vivo. *Glycobiology* 21: 655–662.
71. Ohneda, K., T. Moriguchi, S. Ohmori, Y. Ishijima, H. Satoh, S. Philipsen, and M. Yamamoto. 2014. Transcription factor GATA1 is dispensable for mast cell differentiation in adult mice. *Mol. Cell. Biol.* 34: 1812–1826.
72. Randolph, G. J., J. Ochando, and S. Partida-Sánchez. 2008. Migration of dendritic cell subsets and their precursors. *Annu. Rev. Immunol.* 26: 293–316.
73. Tal, O., H. Y. Lim, I. Gurevich, I. Milo, Z. Shipony, L. G. Ng, V. Angeli, and G. Shakhbar. 2011. DC mobilization from the skin requires docking to immobilized CCL21 on lymphatic endothelium and intralymphatic crawling. *J. Exp. Med.* 208: 2141–2153.
74. Hauser, M. A., I. Kindinger, J. M. Laufer, A. K. Späte, D. Bucher, S. L. Vanes, W. A. Krueger, V. Wittmann, and D. F. Legler. 2016. Distinct CCR7 glycosylation pattern shapes receptor signaling and endocytosis to modulate chemotactic responses. *J. Leukoc. Biol.* 99: 993–1007.
75. Hansen, M., Ö. Met, N. B. Larsen, M. M. Rosenkilde, M. H. Andersen, I. M. Svane, and G. M. Hjortø. 2016. Autocrine CCL19 blocks dendritic cell migration toward weak gradients of CCL21. *Cytotherapy* 18: 1187–1196.
76. Sánchez-Sánchez, N., L. Rioli-Blanco, G. de la Rosa, A. Puig-Kröger, J. García-Bordas, D. Martín, N. Longo, A. Cuadrado, C. Cabañas, A. L. Corbí, et al. 2004. Chemokine receptor CCR7 induces intracellular signaling that inhibits apoptosis of mature dendritic cells. *Blood* 104: 619–625.
77. Britschgi, M. R., S. Favre, and S. A. Luther. 2010. CCL21 is sufficient to mediate DC migration, maturation and function in the absence of CCL19. *Eur. J. Immunol.* 40: 1266–1271.
78. Kiermaier, E., C. Moussion, C. T. Veldkamp, R. Gerardy-Schahn, I. de Vries, L. G. Williams, G. R. Chaffee, A. J. Phillips, F. Freiburger, R. Imre, et al. 2016. Polysialylation controls dendritic cell trafficking by regulating chemokine recognition. *Science* 351: 186–190.
79. Li, Y., and X. Chen. 2012. Sialic acid metabolism and sialyltransferases: natural functions and applications. *Appl. Microbiol. Biotechnol.* 94: 887–905.
80. Crespo, H. J., J. T. Lau, and P. A. Videira. 2013. Dendritic cells: a spot on sialic acid. *Front. Immunol.* 4: 491.
81. Rollenhagen, M., F. F. Buettner, M. Reismann, A. C. Jirno, M. Grove, G. M. Behrens, R. Gerardy-Schahn, F. G. Hanisch, and M. Mühlhoff. 2013. Polysialic acid on neuropilin-2 is exclusively synthesized by the polysialyltransferase ST8SiaIV and attached to mucin-type o-glycans located between the b2 and c domain. *J. Biol. Chem.* 288: 22880–22892.
82. Kiwamoto, T., M. E. Brummet, F. Wu, M. G. Motari, D. F. Smith, R. L. Schnaar, Z. Zhu, and B. S. Bochner. 2014. Mice deficient in the St3gal3 gene product alpha2,3 sialyltransferase (ST3Gal-III) exhibit enhanced allergic eosinophilic airway inflammation. *J. Allergy Clin. Immunol.* 133: 240–247.e1–e3.